
Fast Quantum Algorithm for Learning with Optimized Random Features

Hayata Yamasaki¹ Sathyawageeswar Subramanian² Sho Sonoda³ Masato Koashi^{4,1}

Abstract

Kernel methods augmented with random features give scalable algorithms for learning from big data. But it has been computationally hard to sample random features according to a probability distribution that is optimized for the data, so as to minimize the required number of features for achieving the learning to a desired accuracy. Here, we develop a quantum algorithm for sampling from this optimized distribution over features, in runtime $O(D)$ that is linear in the dimension D of the input data. Our algorithm achieves an exponential speedup in D compared to any known classical algorithm for this sampling task. In contrast to existing quantum machine learning algorithms, our algorithm circumvents sparsity and low-rank assumptions and thus has wide applicability. We also show that the sampled features can be combined with regression by stochastic gradient descent to achieve the learning without canceling out our exponential speedup. Our algorithm based on sampling optimized random features leads to an accelerated framework for machine learning that takes advantage of quantum computers.

1. Introduction

Random features (Rahimi & Recht, 2008) provide a powerful technique for scaling up kernel methods (Schölkopf & Smola, 2001) applicable to various machine learning tasks, such as ridge regression (Rudi & Rosasco, 2017), kernel learning (Sinha & Duchi, 2016), and principle component analysis (Ullah et al., 2018). Recently, Bach (2017) has shown an optimized probability distribution of random features, and sampling features from this optimized distribution would drastically improve runtime of learning algorithms based on random features. However, this sampling task has been computationally “hard in practice” (Bach, 2017) due

to inversion of a high-dimensional operator. In contrast, the power of quantum computers to process data in quantum superposition attracts growing attention towards accelerating learning tasks, opening a new field of quantum machine learning (QML) (Biamonte et al., 2017; Ciliberto et al., 2018; Dunjko & Briegel, 2018). In this work, we develop a framework of QML that accelerates a supervised learning task, by constructing an efficient quantum algorithm for sampling from this optimized distribution.

Learning with random features: Supervised learning deals with the problem of estimating an unknown function $y = f(x)$. We will consider D -dimensional input $x \in \mathbb{R}^D$ and real-valued output $y \in \mathbb{R}$. Given N input-output pairs, we want to learn f to a desired accuracy $\epsilon > 0$. Kernel methods use the reproducing kernel Hilbert space (RKHS) associated with a symmetric, positive semidefinite function $k(x', x)$, the *kernel*, to model the function f (Schölkopf & Smola, 2001). Traditional kernel methods may not be scalable as the number of data N gets large. But random features enable scalable learning algorithms based on kernel methods, along with other techniques for scaling-up via low-rank matrix approximation such as Smola & Schölkopf (2000); Williams & Seeger (2001); Fine & Scheinberg (2002).

Algorithms using random features are based on the fact that we can represent any translation-invariant kernel k as the expectation of a feature map $\varphi(v, x) = e^{-2\pi i v \cdot x}$ over a probability measure $d\tau(v)$ corresponding to the kernel. Conventional algorithms using random features (Rahimi & Recht, 2008; 2009) sample M D -dimensional parameters $v_0, \dots, v_{M-1} \in \mathbb{R}^D$ from the probability distribution $d\tau(v)$ to decide M features $\varphi(v_m, \cdot)$ in time $O(MD)$. For a class of kernels such as Gaussian, this runtime may be reduced to $O(M \log D)$ (Le et al., 2013; Yu et al., 2016). We learn the function f using a linear combination of the M features, i.e.

$$f(x) \approx \sum_{m=0}^{M-1} \alpha_m \varphi(v_m, x) =: \hat{f}(x). \quad (1)$$

To achieve the learning to an accuracy $O(\epsilon)$, we need to settle on a sufficiently large number M of features. Once we fix the M features, we obtain the coefficients α_m by linear (or ridge) regression to minimize an error between f and \hat{f} , using the N data (Rahimi & Recht, 2009; Rudi & Rosasco, 2017; Carratino et al., 2018). By doubly stochastic

¹Photon Science Center, The University of Tokyo, Tokyo, Japan
²DAMTP, University of Cambridge, Cambridge, UK
³RIKEN AIP, Tokyo, Japan
⁴Department of Applied Physics, The University of Tokyo, Tokyo, Japan. Correspondence to: Hayata Yamasaki <yamasaki@qi.t.u-tokyo.ac.jp>.

gradients (Dai et al., 2014), we can perform the sampling of features and the regression of coefficients simultaneously.

Problem: These conventional methods for obtaining random features from the data-independent distribution $d\tau(v)$ require a *large* number M of features to learn the function f , which *slows down* the decision of all M features and the regression over M coefficients. Aiming at minimizing M required for the learning, rather than sampling from $d\tau(v)$, we will sample features from a probability distribution that puts greater weight on *important features that are optimized for the data*, via a probability density function $q(v)$ for $d\tau(v)$. To minimize M achieving the accuracy $O(\epsilon)$, Bach (2017) provides an optimized probability density function $q_\epsilon^*(v)$ for given $d\tau(v)$ (see (3), Sec. 2.1). This optimized $q_\epsilon^*(v)$ achieves minimal M up to a logarithmic gap among all algorithms using random features, for a fixed accuracy ϵ . It *significantly improves* M compared to sampling from $d\tau(v)$ (Bach, 2017; Rudi & Rosasco, 2017; Sun et al., 2018); for example, to achieve learning with the Gaussian kernel from the N data given according to sub-Gaussian distributions, compared to sampling from the data-independent distribution $d\tau(v)$ such as Rahimi & Recht (2008; 2009), the required number M of features sampled from the optimized distribution $q_\epsilon^*(v)d\tau(v)$ can be *exponentially small* in ϵ (Bach, 2017). We call features sampled from $q_\epsilon^*(v)d\tau(v)$ *optimized random features*.

However, sampling from $q_\epsilon^*(v)d\tau(v)$ has been computationally hard in practice owing to two difficulties (Bach, 2017). First, the definition (3) of $q_\epsilon^*(v)$ includes an *infinite-dimensional operator* $(\Sigma + \epsilon\mathbb{1})^{-1}$ on the space of functions $f : \mathbb{R}^D \rightarrow \mathbb{R}$ with D -dimensional input, which is intractable to calculate by computer without approximation. Second, even if we approximate $\Sigma + \epsilon\mathbb{1}$ by an operator on a finite-dimensional space, the *inverse operator* approximating $(\Sigma + \epsilon\mathbb{1})^{-1}$ is still hard to calculate; in particular, for achieving a desired accuracy in the approximation, the required dimension of this finite-dimensional space can be exponentially large in data dimension D , i.e. $O(\exp(D))$ (Sun et al., 2018; Shahrampour & Kolouri, 2019), and *no known algorithm* can calculate the inverse operator on the $O(\exp(D))$ -dimensional space in general *within sub-exponential time* in D .

We note that Avron et al. (2017) propose a probability density function similar to $q_\epsilon^*(v)$, from which the samples can be obtained in polynomial time (Avron et al., 2017; Li et al., 2019; Liu et al., 2019); however, in contrast to sampling from $q_\epsilon^*(v)d\tau(v)$, sampling from the distribution of Avron et al. (2017) does not necessarily minimize the required number M of features for approximating the function f .¹ Simi-

¹The distribution of Avron et al. (2017) and $q_\epsilon^*(v)d\tau(v)$ of Bach (2017) are different in that the former is defined using a Gram matrix of the kernel, but the latter is defined using an integral

operator, whereas sampling from an importance-weighted distribution may also be used in column sampling for scaling-up kernel methods via low-rank matrix approximation, algorithms for the column sampling (Bach, 2013; Alaoui & Mahoney, 2015; Rudi et al., 2018) are not applicable to our setting based on random features; for more detail, we refer to Bach (2017) on the difference between the setting of column sampling and that of sampling random features from $q_\epsilon^*(v)$. Quasi-Monte Carlo techniques (Avron et al., 2016; Chang et al., 2017) also improve M , but it is unknown whether they can achieve minimal M .

Summary of our contributions: As discussed above, the bottleneck in algorithms using random features from the optimized distribution $q_\epsilon^*(v)d\tau(v)$ is each sampling step that works with inversion of $O(\exp(D))$ -dimensional operators for D -dimensional input data. To address this bottleneck and overcome the difficulties in sampling from $q_\epsilon^*(v)d\tau(v)$, we discover that we can use a *quantum algorithm*, rather than conventional classical algorithms that run on existing computers. Our contributions are as follows.

- (Theorem 1) We construct a new quantum algorithm for **sampling an optimized random feature from $q_\epsilon^*(v)d\tau(v)$ in as fast as linear runtime $O(D)$ in the data dimension D** . The best existing classical algorithm by Bach (2017) for sampling each single feature from this *data-optimized* distribution $q_\epsilon^*(v)d\tau(v)$ requires exponential runtime $O(\exp(D))$ (Sun et al., 2018; Shahrampour & Kolouri, 2019). In contrast, our quantum algorithm can sample each single feature from $q_\epsilon^*(v)d\tau(v)$ with runtime $O(D)$, which is as fast as the conventional algorithms such as Rahimi & Recht (2008; 2009). We emphasize that these conventional algorithms perform an easier task, i.e. sampling from a *data-independent* distribution $d\tau(v)$. Advantageously over the conventional algorithms sampling from $d\tau(v)$, we can use our quantum algorithm sampling from $q_\epsilon^*(v)d\tau(v)$ to achieve learning with a significantly small number M of features, which is proven to be *minimal* up to a logarithmic gap (Bach, 2017). Remarkably, we achieve this without assuming sparsity or low rank of relevant operators.
- To construct this quantum algorithm, we **circumvent the difficulty of infinite dimension** by formulating a discrete approximation of the problem of sampling a real-valued feature from $q_\epsilon^*(v)d\tau(v)$. This approxima-

operator as shown in (3). Even if we discretize the integral operator, we do not obtain the Gram matrix. Bach (2017) has proven (near) optimality of sampling from $q_\epsilon^*(v)d\tau(v)$ in minimizing the required number M of features for approximating an arbitrary function f in the model given by RKHS to accuracy $O(\epsilon)$, but this proof of the optimality in the function-approximation setting is not applicable to sampling from the distribution of Avron et al. (2017).

tion is equivalent to using fixed-point number representation with rescaling.

- (Theorem 2) We show that we can combine M features sampled by our algorithm with regression by stochastic gradient descent **to achieve supervised learning in time $O(MD)$, i.e. without canceling out our exponential speedup**. This M is minimal up to a logarithmic gap (Bach, 2017), since we use optimized random features. Thus, by improving the computational bottleneck faced by classical algorithms for sampling optimized random features, we provide a promising framework of quantum machine learning that leverages our $O(D)$ sampling algorithm to achieve the optimal M among all algorithms using random features.

Comparison with previous works on quantum machine learning (QML): The novelty of our contributions is that we construct a QML algorithm that is *free from sparsity or low-rank assumptions* yet achieves an *exponential speedup* compared to any existing classical algorithm using the sampling from the optimized distribution $q_\epsilon^*(v)d\tau(v)$.

Despite major efforts to apply QML to kernel methods (Mengoni & Di Pierro, 2019), super-polynomial speedups like Shor’s algorithm for prime factoring (Shor, 1997) are rare in QML. In fact, it has been challenging to find applications of quantum algorithms with super-polynomial speedups for practical problems (Montanaro, 2016). Typical QML algorithms such as Harrow et al. (2009); Wiebe et al. (2012); Lloyd et al. (2016); Zhao et al. (2019) may achieve exponential speedups over classical algorithms only if matrices involved in the algorithms are sparse; in particular, $n \times n$ matrices can have only $\text{polylog}(n)$ nonzero elements in each row and column. Another class of QML algorithms such as Lloyd et al. (2014); Rebentrost et al. (2014); Kerenidis & Prakash (2017); Wossnig et al. (2018) do not require sparsity but may attain large speedups only if the involved matrices have low rank. This class of quantum algorithms are only polynomially faster than recent “quantum-inspired” classical algorithms such as Tang (2019); Jethwani et al. (2019); Chia et al. (2019), which also assume low rank. Quantum singular value transformation (QSVT) (Gilyén et al., 2019) has recently emerged as a fundamental subroutine that can be used to implement these quantum algorithms in a unified way. However, these assumptions restrict the power and the applicability of the QML algorithms (Aaronson, 2015).

Our key technical contribution is to develop a fast QML algorithm that circumvents the sparsity and low-rank assumptions, broadening the applicability of QML. We achieve this by combining the QSVT with another subroutine, the quantum Fourier transform (QFT) (Hales & Hallgren, 2000). QFT and QSVT are broadly used as fundamental subroutines in quantum computation (Nielsen & Chuang, 2011;

de Wolf, 2019). However, it is nontrivial how to use these subroutines, QFT and QSVT, to develop a QML algorithm that exponentially outperforms existing classical algorithms *under widely applicable assumptions*. In achieving the speedup, our technique avoids the sparsity and low-rank assumptions by decomposing the $O(\exp(D))$ -dimensional *fully dense (i.e. non-sparse) and full-rank* operator representing $\Sigma + \epsilon \mathbb{1}$ in the definition (3) of $q_\epsilon^*(v)$ into diagonal (i.e. sparse) operators using Fourier transform. The powerful subroutines may make our algorithm hard to simulate numerically by classical computation, and hard to perform even on near-term quantum computers (Havlíček et al., 2019; Arute et al., 2019) that cannot implement universal quantum computation due to noise. For this reason, this paper does not include numerical simulation, and we analytically prove that the runtime of our quantum algorithm is as fast as linear in D . The wide applicability of our algorithm makes it a promising candidate for “killer applications” of universal quantum computers.

2. Preliminaries

2.1. Supervised learning by optimized random features

We introduce the supervised learning setting that we focus on in this paper, and we will formulate an approximate version of it in Sec. 3. Suppose that N pairs of data are given $(x_0, y_0), \dots, (x_{N-1}, y_{N-1}) \in \mathcal{X} \times \mathcal{Y}$, where $y_n = f(x_n)$, $f: \mathcal{X} \rightarrow \mathcal{Y}$ is an unknown function to be learned, $\mathcal{X} = \mathbb{R}^D$ is the domain for D -dimensional input data, $\mathcal{Y} = \mathbb{R}$ is the range for output data. Each x_n is an observation of an independently and identically distributed (IID) random variable on \mathcal{X} equipped with a probability measure $d\rho(x) = q^{(\rho)}(x)dx$. We choose a translation-invariant kernel; any such kernel can be represented as

$$k(x', x) = k_{\text{TI}}(x' - x) = \int d\tau(v) \overline{\varphi(v, x')} \varphi(v, x), \quad (2)$$

where $\bar{\cdot}$ is complex conjugation, $\varphi: \mathcal{V} \times \mathcal{X} \rightarrow \mathbb{C}$ is a feature map $\varphi(v, x) = e^{-2\pi i v \cdot x}$, $\mathcal{V} = \mathbb{R}^D$ is a parameter space equipped with a probability measure $d\tau(v) = q^{(\tau)}(v)dv$, and $d\tau(v)$ is given by the Fourier transform of k_{TI} (Rahimi & Recht, 2008). The kernel is normalized by $k(0, 0) = \int_{\mathcal{V}} d\tau(v) = 1$. To specify a model of f , we use the reproducing kernel Hilbert space \mathcal{F} (RKHS) associated with the kernel k .² We aim to learn an estimate of f from the given data, so that the generalization error between f and our estimate can be bounded to a desired accuracy $\epsilon > 0$.

To achieve this learning to the accuracy $O(\epsilon)$ with the minimal number M of random features, rather than sampling from $d\tau$, Bach (2017) proposes to sample features according

²We assume that the norm $\|f\|_{\mathcal{F}}$ of f on the RKHS is bounded, in particular, $\|f\|_{\mathcal{F}} \leq 1$, to use the result of Bach (2017).

to an optimized probability density function q_ϵ^* for $d\tau$

$$q_\epsilon^*(v) \propto \langle \varphi(v, \cdot) | (\Sigma + \epsilon \mathbb{1})^{-1} \varphi(v, \cdot) \rangle_{L_2(d\rho)}, \quad (3)$$

where $\langle f | g \rangle_{L_2(d\rho)} := \int_{\mathcal{X}} d\rho(x) \overline{f(x)} g(x)$, $\mathbb{1}$ is the identity operator, $\Sigma : L_2(d\rho) \rightarrow L_2(d\rho)$ is the integral operator $(\Sigma f)(x') := \int_{\mathcal{X}} d\rho(x) k(x', x) f(x)$ (Cucker & Smale, 2002), and q_ϵ^* is normalized by $\int_{\mathcal{V}} q_\epsilon^*(v) d\tau(v) = 1$. The function $q_\epsilon^*(v)$ is called a leverage score.

Indeed, Bach (2017) shows that for any f satisfying $\|f\|_{\mathcal{F}} \leq 1$, it suffices to sample $M = O(d(\epsilon) \log(d(\epsilon)/\delta))$ features from $q_\epsilon^*(v) d\tau(v)$ to achieve

$$\min_{\alpha} \left\{ \int_{\mathcal{X}} d\rho(x) \left| f(x) - \sum_{m=0}^{M-1} \alpha_m \varphi(v_m, x) \right|^2 \right\} \leq 4\epsilon \quad (4)$$

with probability greater than $1 - \delta$, where $d(\epsilon) := \text{Tr} \Sigma (\Sigma + \epsilon \mathbb{1})^{-1}$ is the degree of freedom representing effective dimension of data. As a prerequisite of using any kernel method, regardless of using random features or low-rank matrix approximation, the kernel k should be suitably chosen for learning data from the distribution $d\rho$; otherwise, it is impossible for the kernel methods to achieve the learning with reasonable runtime and accuracy. In the case of random features, to guarantee $M = O(\text{poly}(D, 1/\epsilon))$, we assume

$$d(\epsilon) = O(\text{poly}(D, 1/\epsilon)), \quad (5)$$

where $d(\epsilon)$ depends on Σ and hence on both $d\rho$ and k that should be chosen suitably to satisfy (5); otherwise, f may not have a polynomial-size description in terms of the features.

We call features sampled from $q_\epsilon^*(v) d\tau(v)$ up to an approximation *optimized random features*, which nearly minimize M required for the learning as discussed in Sec. 1.

2.2. Quantum computation

We now summarize the basic notions and notations of quantum computation required to describe our quantum algorithms, referring to Nielsen & Chuang (2011); de Wolf (2019) for more detail.

The basic unit of a quantum computer, analogous to the classical bit taking states $b \in \{0, 1\}$, is a *qubit* taking *quantum states* $|\psi\rangle = \alpha_0 |0\rangle + \alpha_1 |1\rangle := \begin{pmatrix} \alpha_0 \\ \alpha_1 \end{pmatrix} \in \mathbb{C}^2$, where $\{|0\rangle := \begin{pmatrix} 1 \\ 0 \end{pmatrix}, |1\rangle := \begin{pmatrix} 0 \\ 1 \end{pmatrix}\}$. While an m -bit register takes values in $\{0, 1\}^m$, an m -qubit register takes states $|\psi\rangle = \sum_{x=0}^{2^m-1} \alpha_x |x\rangle$ in the 2^m -dimensional tensor product Hilbert space $\mathcal{H} = (\mathbb{C}^2)^{\otimes m} = \mathbb{C}^{2^m}$. We call a fixed orthonormal basis $\{|x\rangle : x \in \{0, \dots, 2^m - 1\}\}$ labeled by m -bit strings or the corresponding integers, the *computational basis* of \mathcal{H} .

Quantum states $|\psi\rangle$ require an L_2 normalization condition: $\| |\psi\rangle \|_2 = \sum_{x=0}^{2^m-1} |\alpha_x|^2 = 1$, which enables us to interpret $|\alpha_x|^2$ as probability. A *measurement* on an m -qubit state $|\psi\rangle$ in the computational basis is a sampling process that returns a randomly chosen m -bit string x with probability $p(x) = |\alpha_x|^2$. We defer further detail regarding measurements to our Supplementary Materials.

The conjugate transpose of a column vector $|\psi\rangle$ is a row vector denoted by $\langle \psi|$. The conjugate transpose and the transpose of an operator \mathbf{A} are denoted by \mathbf{A}^\dagger and \mathbf{A}^T , respectively. The inner product of $|\psi\rangle$ and $|\phi\rangle$ is denoted by $\langle \psi | \phi \rangle$, while their outer product $|\psi\rangle \langle \phi|$ is a matrix.

A quantum algorithm starts by initializing m qubits in a fixed state $|0\rangle^{\otimes m}$, which we may write as $|0\rangle$ if m is obvious from context. Then, we apply a 2^m -dimensional unitary operator \mathbf{U} to $|0\rangle^{\otimes m}$, to prepare a state $\mathbf{U} |0\rangle^{\otimes m}$. Finally, a measurement on $\mathbf{U} |0\rangle^{\otimes m}$ is performed to sample an m -bit string from the probability distribution given by $\mathbf{U} |0\rangle^{\otimes m}$. Analogously to classical logic circuits, \mathbf{U} is represented by a quantum circuit composed of sequential applications of unitaries acting on at most two qubits at a time, which are called (elementary) quantum gates. With techniques shown in Subramanian et al. (2019); Chakraborty et al. (2018); Gilyén et al. (2019), non-unitary operators can also be implemented in quantum computation. In particular, to implement a non-unitary operator \mathbf{A} , we will use the technique of *block encodings* (Gilyén et al., 2019) in this paper.³ The runtime of a quantum algorithm is determined by the number of elementary quantum gates in its circuit.

3. Setting for sampling random feature

3.1. Discretization of real number

To clarify our setting of digital quantum computation, we explain how to represent real numbers in our quantum algorithm. We assume that the input data domain is bounded; in particular, the space where $d\rho(x) > 0$ is $[0, x_{\max}]^D$ for some $x_{\max} > 0$. If the kernel $k(x', x)$ is a function decaying to 0 sufficiently fast as x' and x deviate from 0, such as Gaussian, we can take $G \gg x_{\max}$ to approximate $k(x', x)$

³A block encoding of \mathbf{A} is a unitary operator $\mathbf{U} = \begin{pmatrix} \mathbf{A} & \\ & \cdot \end{pmatrix}$ that encodes \mathbf{A} in its top-left (or $|0\rangle \langle 0|$) subspace. Suppose that we apply \mathbf{U} to a state $|0\rangle \otimes |\psi\rangle = \begin{pmatrix} |\psi\rangle \\ \mathbf{0} \end{pmatrix}$, where $\mathbf{0}$ is a zero column vector, and $|0\rangle \in \mathbb{C}^d$ for some d . Then, we obtain $\mathbf{U}(|0\rangle \otimes |\psi\rangle) = \sqrt{p} |0\rangle \otimes \frac{\mathbf{A}|\psi\rangle}{\|\mathbf{A}|\psi\rangle\|_2} + \sqrt{1-p} |\perp\rangle$, where $p = \|\mathbf{A}|\psi\rangle\|_2^2$. The state $|\perp\rangle$ satisfies $\langle 0 | \langle 0 | \mathbb{1} | \perp \rangle = 0$ and is of no interest. We can prepare the state $\frac{\mathbf{A}|\psi\rangle}{\|\mathbf{A}|\psi\rangle\|_2}$ with high probability using this process for preparing $\mathbf{U}(|0\rangle \otimes |\psi\rangle)$ (and its inverse) repeatedly $O(1/\sqrt{p})$ times, by means of *amplitude amplification* (Brassard et al., 2002).

Table 1. How to rescale data by a parameter $r > 1$.

Original data and functions	Rescaled by $r > 1$
Upper bound G of interval $[0, G]$	$G_r = rG$
Kernel $\tilde{k}(x', x)$	$\tilde{k}_r(rx', rx) := \tilde{k}(x', x)$
Input x	rx
Output $y = f(x)$ to be learned	$y = f_r(rx) := f(x)$
Data distribution $q^{(\rho)}(x)dx = d\rho(x)$	$q_r^{(\rho)}(rx) := q^{(\rho)}(x)/r$
Lipschitz constant $L^{(f)}$ of $f(x)$	$L_r^{(f_r)} = L^{(f)}/r$
Lipschitz constant $L^{(q^{(\rho)})}$ of $q^{(\rho)}(x)$	$L_r^{(q_r^{(\rho)})} = L^{(q^{(\rho)})}/r^2$

for any $\tilde{x}, x \in [0, x_{\max}]^D$ using a (periodic) function \tilde{k}

$$k(x', x) \approx \sum_{n \in \mathbb{Z}^D} k(x', x + Gn) =: \tilde{k}(x', x). \quad (6)$$

We will use \tilde{k} as a kernel in place of k . In computation, it is usual to represent a real number using a finite number of bits; e.g., fixed-point number representation with small precision $\Delta > 0$ uses a finite set $\{0, \Delta, 2\Delta, \dots, G - \Delta\}$ to represent a real interval $[0, G]$. Equivalently, to simplify the presentation, we use the fixed-point number representation rescaled by a parameter $r = 1/\Delta$ as shown in Table 1, so that we can use a set of integers $\mathcal{I} = \{0, 1, \dots, G_r - 1\}$ to discretize the interval.

We represent the data domain $\mathcal{X} = \mathbb{R}^D$ as $\tilde{\mathcal{X}} = \mathcal{I}^D$. Discretization of the data range \mathcal{Y} is unnecessary in this paper. For any real-valued point $x \in \mathcal{X}$, we write its closest grid point as $\tilde{x} \in \tilde{\mathcal{X}}$, and let $\Delta_x \subset \mathbb{R}^D$ denote a D -dimensional unit hypercube whose center is the closest grid point \tilde{x} to x .

To justify this discretization, we assume that functions in the learning, such as the function f to be learned and the probability density $q^{(\rho)}(x)$ of data, are L -Lipschitz continuous for some Lipschitz constant L .⁴ Then, errors caused by discretization, such as $|f(x) - f(\tilde{x})|$ and $|q^{(\rho)}(x) - q^{(\rho)}(\tilde{x})|$, are negligible in the limit of small (but still nonzero) Lipschitz constant $L\sqrt{D} \rightarrow 0$ as the data dimension D gets large. We reduce these errors by rescaling the data to a larger domain (see Table 1); in particular, to reduce $L\sqrt{D}$ to a fixed error threshold, we need to rescale G representing the interval $[0, G]$ to $G_r = \Omega(L\sqrt{D})$. This rescaling keeps the accuracy and the model in the learning *invariant*.

We focus on asymptotic runtime analysis of our algorithm as G_r gets larger, to reduce the errors in the discretization. We henceforth omit the subscript r and write G_r as G for brevity. An error analysis of discretization for finite G is out of the scope of this paper; for such an analysis, we refer to established procedures in signal processing (Proakis, 2001).

As we can represent $\tilde{\mathcal{X}}$ using $D \lceil \log_2 G \rceil$ bits, where $\lceil x \rceil$ is the least integer greater than or equal to x , we similarly

⁴For any $x, x' \in \mathcal{X}$, a function $q : \mathcal{X} \rightarrow \mathbb{C}$ is L -Lipschitz continuous if it holds that $|q(x) - q(x')| \leq L\|x - x'\|_2$.

 Table 2. Discretized representation of \mathcal{X} by \mathcal{H}^X . Note $\tilde{x}', \tilde{x} \in \tilde{\mathcal{X}}$.

Function / operator on \mathcal{X}	Vector / operator on \mathcal{H}^X
$f : \mathcal{X} \rightarrow \mathbb{C}$	$ f\rangle := \sum_{\tilde{x}} f(\tilde{x}) \tilde{x}\rangle$
$\varphi(v, \cdot) : \mathcal{X} \rightarrow \mathbb{C}$	$ \varphi(v, \cdot)\rangle := \sum_{\tilde{x}} \varphi(v, \tilde{x}) \tilde{x}\rangle$
$\tilde{k} : \mathcal{X} \times \mathcal{X} \rightarrow \mathbb{R}$	$\mathbf{k} := \sum_{\tilde{x}', \tilde{x}} \tilde{k}(\tilde{x}', \tilde{x}) \tilde{x}'\rangle \langle \tilde{x} $
$q^{(\rho)} : \mathcal{X} \rightarrow \mathbb{R}$	$\mathbf{q}^{(\rho)} := \sum_{\tilde{x}} q^{(\rho)}(\tilde{x}) \tilde{x}\rangle \langle \tilde{x} $
Σ acting on $f : \mathcal{X} \rightarrow \mathbb{C}$	$\mathbf{\Sigma} := \mathbf{k}\mathbf{q}^{(\rho)}$
$\Sigma f : \mathcal{X} \rightarrow \mathbb{C}$	$\mathbf{\Sigma} f\rangle$

represent $\tilde{\mathcal{X}}$ using a quantum register of $D \lceil \log_2 G \rceil$ qubits

$$\mathcal{H}^X := \text{span}\{|\tilde{x}\rangle : \tilde{x} \in \tilde{\mathcal{X}}\}. \quad (7)$$

This quantum register is composed of D sub-registers, i.e. $\mathcal{H}^X = (\mathcal{H}_{\mathcal{I}})^{\otimes D}$, where each sub-register $\mathcal{H}_{\mathcal{I}} = (\mathbb{C}^2)^{\otimes \lceil \log_2 G \rceil}$ corresponds to \mathcal{I} . To represent $\tilde{x} = (\tilde{x}^{(1)}, \dots, \tilde{x}^{(D)})^T \in \tilde{\mathcal{X}}$, we use a quantum state $|\tilde{x}\rangle^X = \bigotimes_{d=1}^D |\tilde{x}^{(d)}\rangle \in \mathcal{H}^X$, where $|\tilde{x}^{(d)}\rangle \in \mathcal{H}_{\mathcal{I}}$.

We represent a function on the continuous space \mathcal{X} as a vector on finite-dimensional \mathcal{H}^X , and an operator acting on functions on \mathcal{X} as a matrix on \mathcal{H}^X , as shown in Table 2. Under our assumption that the rescaling makes the Lipschitz constants sufficiently small, we can make an approximation

$$\langle f | \mathbf{q}^{(\rho)} | g \rangle \approx \int_{\mathcal{X}} d\rho(x) \overline{f(x)} g(x), \quad q^{(\rho)}(x)dx = d\rho(x). \quad (8)$$

With this discretization, we can represent the optimized probability density function q_{ϵ}^* in (3) as

$$\tilde{q}_{\epsilon}^*(v) \propto \langle \varphi(v, \cdot) | \mathbf{q}^{(\rho)} (\mathbf{\Sigma} + \epsilon \mathbb{1})^{-1} | \varphi(v, \cdot) \rangle, \quad (9)$$

where \tilde{q}_{ϵ}^* is normalized by $\int_{\mathcal{Y}} \tilde{q}_{\epsilon}^*(v) d\tau(v) = 1$.

3.2. Data in discretized representation

To represent the real-valued input data $x_n \in \mathcal{X}$ that is IID sampled according to the probability measure $d\rho(x)$, we use discretization. We represent x_n using its closest grid point $\tilde{x}_n \in \tilde{\mathcal{X}}$, IID sampled with probability $\int_{\Delta_{x_n}} d\rho(x)$, where Δ_{x_n} is the D -dimensional unit hypercube centered at x_n . In the following, the N pairs of given data are $(\tilde{x}_0, y_0), \dots, (\tilde{x}_{N-1}, y_{N-1}) \in \tilde{\mathcal{X}} \times \mathcal{Y}$, where $y_n = f(\tilde{x}_n)$.

The true probability distribution $d\rho$ of the data is unknown in our setting, and our algorithm uses the N given data to calculate an operator that represents $d\rho(x) = q^{(\rho)}(x)dx$ approximately up to a statistical error. For any $\tilde{x} \in \tilde{\mathcal{X}}$, let $n(\tilde{x})$ denote the number of given data that are included in the D -dimensional unit hypercube $\Delta_{\tilde{x}}$. We approximate the distribution $d\rho$ near \tilde{x} by an empirical distribution counting the data: $\hat{q}^{(\rho)}(\tilde{x}) := n(\tilde{x})/N$. In the same way as $\mathbf{\Sigma} = \mathbf{k}\mathbf{q}^{(\rho)}$ in Table 2, an empirical integral operator is given by

$$\hat{\mathbf{\Sigma}} := \mathbf{k}\hat{\mathbf{q}}^{(\rho)}, \quad \hat{\mathbf{q}}^{(\rho)} := \sum_{\tilde{x} \in \tilde{\mathcal{X}}} \hat{q}^{(\rho)}(\tilde{x}) |\tilde{x}\rangle \langle \tilde{x}|. \quad (10)$$

We aim to analyze the asymptotic runtime of our algorithm when the number N of data points becomes large, as with large G for rescaling. In the limit $N \rightarrow \infty$, statistical errors in the empirical distribution caused by the finiteness of N vanish. Analysis of statistical errors for finite N is out of the scope of this paper; for such an analysis, see Bach (2017).

3.3. Input model

The time required for accessing data is a matter of computational architecture and data structure. Whereas Turing machines can only access data sequentially, modern computers actually have random access memory (RAM). Thus, it is reasonable to introduce a model of inputting data to our algorithm based on RAM. Abstracting implementations of the RAM, we assume access to the n th data via oracles

$$\mathcal{O}_{\tilde{x}}(n) = \tilde{x}_n, \quad \mathcal{O}_y(n) = y_n, \quad (11)$$

which are functions that map each $n \in \{0, \dots, N-1\}$ to the data. The runtimes for each query to $\mathcal{O}_{\tilde{x}}$ and \mathcal{O}_y are denoted by $T_{\tilde{x}}$ and T_y , respectively.

Analogously to sampling \tilde{x} with probability $\hat{q}(\tilde{x})$, we allow a quantum computer to use a quantum oracle (i.e. a unitary) \mathcal{O}_ρ to set a quantum register \mathcal{H}^X to a quantum state

$$\mathcal{O}_\rho(|0\rangle) = \sum_{\tilde{x} \in \tilde{\mathcal{X}}} \sqrt{\hat{q}(\tilde{x})} |\tilde{x}\rangle = \sqrt{\hat{\mathbf{q}}^{(\rho)}} \sum_{\tilde{x} \in \tilde{\mathcal{X}}} |\tilde{x}\rangle, \quad (12)$$

so that we can sample \tilde{x} with probability $\hat{q}(\tilde{x})$ by a measurement on this state in the computational basis $\{|\tilde{x}\rangle\}$. Note that for an operator \mathbf{A} , $f(\mathbf{A})$ is an operator given by applying f to the singular values of \mathbf{A} while keeping the singular vectors, i.e. $\sqrt{\hat{\mathbf{q}}^{(\rho)}} = \sum_{\tilde{x} \in \tilde{\mathcal{X}}} \sqrt{\hat{q}(\tilde{x})} |\tilde{x}\rangle \langle \tilde{x}|$.

Abstracting implementations of \mathcal{O}_ρ ,⁵ we let T_ρ denote the runtime for each query to \mathcal{O}_ρ . We assume that both \mathcal{O}_ρ and

⁵We can efficiently implement the oracle \mathcal{O}_ρ with an acceptable preprocessing overhead, using the N given data points $\tilde{x}_0, \dots, \tilde{x}_{N-1}$. From the data, we can prepare a data structure proposed by Kerenidis & Prakash (2017) in $O(N(D \log G)^2)$ time using $O(N(D \log G)^2)$ bits of memory, while collecting and storing the N data points requires at least $\Theta(ND \log G)$ time and $\Theta(ND \log G)$ bits of memory. Then, we can implement \mathcal{O}_ρ by a quantum circuit combined with a quantum random access memory (QRAM) (Giovannetti et al., 2008a;b), which can load data from this data structure into qubits in quantum superposition (i.e. linear combinations of quantum states). With T denoting runtime of this QRAM per query, it is known that this implementation of \mathcal{O}_ρ with precision Δ has runtime $T_\rho = O(D \log(G) \text{polylog}(1/\Delta) \times T)$ per query (Grover & Rudolph, 2002). We do not include the time for collecting the data or preparing the above data structure in runtime of our learning algorithm. The use of QRAM is a common assumption in QML especially to deal with a large amount of data; however, even with QRAM, achieving quantum speedup is nontrivial. Similarly to quantum computers, QRAM is actively under development towards its physical realization; e.g. see Jiang et al. (2019); Hann et al. (2019). In this paper, we assume that both the quantum computer and the QRAM are available.

its inverse \mathcal{O}_ρ^\dagger have the same runtime T_ρ , since \mathcal{O}_ρ^\dagger can be implemented by replacing each quantum gate in the circuit for \mathcal{O}_ρ with its inverse. We note that the number of data points N will not explicitly appear in the runtime of our algorithm, except that the runtimes $T_{\tilde{x}}$, T_y , and T_ρ of the oracles for accessing the data may depend on N .

4. Main results

We now describe our main contribution, an efficient quantum algorithm for sampling an optimized random feature, in our discretized setting of Sec. 3. Algorithm 1 in Sec. 4.1 shows our algorithm, and Theorem 1 bounds its runtime. As we show in Sec. 4.2, it is crucial for our algorithm to use the *perfect reconstruction* of the kernel, i.e., an exact representation of the kernel on the data domain as the *finite* sum of the feature map φ weighted by a function $Q^{(\tau)}(v_G)$ over a *finite* set of features $v_G \in \mathcal{V}_G$ (Proposition 1). Like the diagonal operator $\mathbf{q}^{(\rho)}$ in Table 1, we will define a diagonal operator for $Q^{(\tau)}(v_G)$ as $\mathbf{Q}^{(\tau)}$, the maximum of $Q^{(\tau)}(v_G)$ as $Q_{\max}^{(\tau)}$, and a probability mass function on \mathcal{V}_G proportional to $Q^{(\tau)}(v_G)$ as $P^{(\tau)}(v_G)$. In Sec. 4.3, we clarify how to input this representation of the kernel to our algorithm, by constructing a quantum oracle \mathcal{O}_τ with runtime T_τ . In Sec. 4.4, correspondingly to the optimized distribution $\tilde{q}_\epsilon^*(v) d\tau(v)$ of real-valued features in \mathcal{V} , we provide an optimized probability distribution $Q_\epsilon^*(v_G)P^{(\tau)}(v_G)$ of our features in the finite set \mathcal{V}_G , and construct a quantum state $|\Psi\rangle$ to sample the optimized random feature from $Q_\epsilon^*(v_G)P^{(\tau)}(v_G)$ (Proposition 2). In Algorithm 1, we efficiently prepare the state $|\Psi\rangle$, and perform a measurement on $|\Psi\rangle$ to achieve the sampling. In Sec. 4.5, we also show that we can achieve the learning as a whole without canceling out our quantum speedup by performing linear regression using stochastic gradient descent (Theorem 2).

4.1. Algorithm for sampling optimized random feature

We bound the runtime of our quantum algorithm, Algorithm 1, for sampling an optimized random feature from $Q_\epsilon^*P^{(\tau)}$. The difficulty of sampling from $Q_\epsilon^*P^{(\tau)}$ arises from the fact that the quantum state $|\Psi\rangle$ required for this sampling (see Proposition 2, Sec. 4.4) includes a G^D -dimensional operator $\hat{\Sigma}_\epsilon^{-\frac{1}{2}}$, i.e. on an exponentially large space in D , and $\hat{\Sigma}_\epsilon$ may not be sparse or of low rank. Given an efficient implementation of a block encoding of $\hat{\Sigma}_\epsilon$, quantum singular value transformation (QSVT) (Gilyén et al., 2019) gives an efficient way to implement a block encoding of $\hat{\Sigma}_\epsilon^{-\frac{1}{2}}$ to prepare $|\Psi\rangle$. However, it is not straightforward to discover such an efficient implementation for $\hat{\Sigma}_\epsilon$, as long as we use conventional ways for efficiently implementing block encodings of sparse or low-rank operators such as the diagonal operator $\sqrt{(1/Q_{\max}^{(\tau)})\mathbf{Q}^{(\tau)}}$ (Gilyén et al., 2019).

Algorithm 1 Quantum algorithm for sampling an optimized random feature (quOptRF).

Input: A desired accuracy $\epsilon > 0$ in the supervised learning, sampling precision $\Delta > 0$, quantum oracles \mathcal{O}_ρ in (12) and \mathcal{O}_τ in (19), and $Q_{\max}^{(\tau)} > 0$ in (18).

Output: An optimized random feature $v_G \in \mathcal{V}_G$ sampled from a probability distribution $Q(v_G)P^{(\tau)}(v_G)$ with $\sum_{v_G \in \mathcal{V}_G} |Q(v_G)P^{(\tau)}(v_G) - Q_\epsilon^*(v_G)P^{(\tau)}(v_G)| \leq \Delta$.

- 1: Initialize quantum registers X and X' , and load data $|0\rangle^X \otimes |0\rangle^{X'} \mapsto \sum_{\tilde{x} \in \tilde{\mathcal{X}}} |\tilde{x}\rangle^X \otimes \sqrt{\hat{\mathbf{q}}^{(\rho)}} |\tilde{x}\rangle^{X'}$.
- 2: Perform a D -dimensional quantum Fourier transform \mathbf{F}_D^\dagger on X' to obtain $\sum_{\tilde{x} \in \tilde{\mathcal{X}}} |\tilde{x}\rangle^X \otimes \mathbf{F}_D^\dagger \sqrt{\hat{\mathbf{q}}^{(\rho)}} |\tilde{x}\rangle^{X'}$.
- 3: Apply the block encoding of $\sqrt{(1/Q_{\max}^{(\tau)})\mathbf{Q}^{(\tau)}}$ to X' followed by amplitude amplification to obtain a state proportional to $\sum_{\tilde{x} \in \tilde{\mathcal{X}}} |\tilde{x}\rangle^X \otimes \sqrt{(1/Q_{\max}^{(\tau)})\mathbf{Q}^{(\tau)}} \mathbf{F}_D^\dagger \sqrt{\hat{\mathbf{q}}^{(\rho)}} |\tilde{x}\rangle^{X'}$.
- 4: Apply the block encoding of $\hat{\Sigma}_\epsilon^{-\frac{1}{2}}$ to X to obtain the quantum state $|\Psi\rangle^{XX'}$ in Proposition 2.
- 5: Perform a measurement of X' in the computational basis to obtain \tilde{x} with probability $Q_\epsilon^*(\tilde{x}/G)P^{(\tau)}(\tilde{x}/G)$.
- 6: **Return** $v_G = \tilde{x}/G$.

Recent techniques for ‘‘quantum-inspired’’ classical algorithms (Tang, 2019) are not applicable either, since the full-rank operator $\hat{\Sigma}_\epsilon$ does not have a low-rank approximation.

Our significant technical contribution is to overcome this difficulty by constructing an efficient block encoding of $\hat{\Sigma}_\epsilon$ using quantum Fourier transform (QFT). Using the perfect reconstruction of the kernel (see Proposition 1, Sec. 4.2), we explicitly decompose $\hat{\Sigma}_\epsilon$ into building blocks, i.e., diagonal operators $\sqrt{(1/Q_{\max}^{(\tau)})\mathbf{Q}^{(\tau)}}$, $\sqrt{\hat{\mathbf{q}}^{(\rho)}}$ (efficiently implementable by block encodings), and unitary operators \mathbf{F}_D , \mathbf{F}_D^\dagger representing D -dimensional discrete Fourier transform⁶ and its inverse. The QFT provides a quantum circuit implementing \mathbf{F}_D (and \mathbf{F}_D^\dagger) with precision Δ within time $O(D \log(G) \log \log(G) \text{polylog}(1/\Delta))$ (Hales & Hallgren, 2000). We combine these building blocks to obtain a quantum circuit that efficiently implements the block encoding of $\hat{\Sigma}_\epsilon$. The QSVT of our block encoding of $\hat{\Sigma}_\epsilon$ yields a block encoding of $\hat{\Sigma}_\epsilon^{-\frac{1}{2}}$ with precision Δ , using the block encoding of $\hat{\Sigma}_\epsilon$ repeatedly $\tilde{O}((Q_{\max}^{(\tau)}/\epsilon) \text{polylog}(1/\Delta))$ times (Gilyén et al., 2019), where $Q_{\max}^{(\tau)}/\epsilon$ is the condition number of $\hat{\Sigma}_\epsilon$, and \tilde{O} may ignore poly-logarithmic factors. Then, we achieve the following runtime of Algorithm 1 that is linear in D , whereas no existing algorithm can achieve this sampling in sub-exponential time as discussed in Sec. 1.

Theorem 1 (Runtime of our quantum algorithm for sampling an optimized random feature). *Given D -dimensional*

⁶With \mathbf{F} denoting a unitary operator of (one-dimensional) discrete Fourier transform, we define $\mathbf{F}_D := \mathbf{F}^{\otimes D}$.

Table 3. Distribution function $Q^{(\tau)}(v_G)$ corresponding to the Gaussian kernel (top) and the Laplacian kernel (bottom), where $v_G = (v_G^{(1)}, \dots, v_G^{(D)})^\top$, and ϑ is the theta function defined as $\vartheta(u; q) := 1 + 2 \sum_{n=1}^{\infty} q^{n^2} \cos(2nu)$.

$k(x', x)$	$Q^{(\tau)}(v_G)$
$\exp(-\gamma \ x' - x\ _2^2)$	$\prod_{d=1}^D \vartheta(\pi v_G^{(d)}; e^{-\gamma})$
$\exp(-\gamma \ x' - x\ _1)$	$\prod_{d=1}^D \frac{\sinh(\gamma)}{\cosh(\gamma) - \cos(2\pi v_G^{(d)})}$

data discretized by $G > 0$, for any accuracy $\epsilon > 0$ and any sampling precision $\Delta > 0$, Algorithm 1 samples a feature $v_G \in \mathcal{V}_G$ from a weighted distribution $Q(v_G)P^{(\tau)}(v_G)$ with $\sum_{v_G \in \mathcal{V}_G} |(Q(v_G) - Q_\epsilon^(v_G))P^{(\tau)}(v_G)| \leq \Delta$, in runtime*

$$T_1 = O(D \log(G) \log \log(G) + T_\rho + T_\tau) \times \tilde{O}((Q_{\max}^{(\tau)}/\epsilon) \text{polylog}(1/\Delta)),$$

where T_ρ and T_τ are the runtimes of the oracles \mathcal{O}_ρ and \mathcal{O}_τ per query, and $Q_{\max}^{(\tau)}$ and \mathcal{O}_τ will be defined as (18) and (19), respectively. In particular, T_1 is linear in D .

4.2. Perfect reconstruction of kernel

We describe the crucial technique in our quantum algorithm, i.e., the perfect reconstruction of the kernel. In the same way as representing the kernel k as the expectation (2) of $\varphi(v, x) = e^{-2\pi i v \cdot x}$ over the probability distribution $d\tau = q^{(\tau)}(v)dv$, from Shannon’s sampling theorem (Shannon, 1949) in signal processing, we obtain an exact representation of our kernel \tilde{k} as

$$\tilde{k}(x', x) = \sum_{\tilde{v} \in \mathbb{Z}^D} (q^{(\tau)(\tilde{v}/G)/G^D} \overline{\varphi(\tilde{v}/G, x')} \varphi(\tilde{v}/G, x)). \quad (13)$$

Moreover, we show that to exactly represent \tilde{k} on our discrete data domain, it suffices to use a finite set \mathcal{V}_G of features and a distribution function $Q^{(\tau)}$ over the finite set \mathcal{V}_G

$$v_G \in \mathcal{V}_G := \{0, 1/G, \dots, 1 - 1/G\}^D, \quad (14)$$

$$Q^{(\tau)}(v_G) := \sum_{\tilde{v}' \in \mathbb{Z}^D} q^{(\tau)}(v_G + \tilde{v}'). \quad (15)$$

We give examples of $Q^{(\tau)}$ in Table 3. A diagonal operator corresponding to $Q^{(\tau)}(v_G)$ is given by

$$\mathbf{Q}^{(\tau)} := \sum_{\tilde{x} \in \tilde{\mathcal{X}}} Q^{(\tau)}(v_G) |\tilde{x}\rangle \langle \tilde{x}|, \quad (v_G = \tilde{x}/G). \quad (16)$$

We will use one-to-one correspondence between $v_G \in \mathcal{V}_G$ and $\tilde{x} \in \tilde{\mathcal{X}} = \{0, 1, \dots, G-1\}^D$ given by $v_G = \tilde{x}/G$. We combine $\mathbf{Q}^{(\tau)}$ with the discrete Fourier transform \mathbf{F}_D to obtain the following perfect reconstruction of \tilde{k} .

Proposition 1 (Perfect reconstruction of kernel). *Given any (periodic) translation-invariant kernel \tilde{k} given by (6), we*

exactly have for each $\tilde{x}', \tilde{x} \in \tilde{\mathcal{X}}$

$$\begin{aligned} \tilde{k}(\tilde{x}', \tilde{x}) &= \sum_{v_G \in \mathcal{V}_G} (Q^{(\tau)}(v_G)/G^D) \overline{\varphi(v_G, \tilde{x}')} \varphi(v_G, \tilde{x}) \\ &= \langle \tilde{x}' | \mathbf{F}_D^\dagger \mathbf{Q}^{(\tau)} \mathbf{F}_D | \tilde{x} \rangle = \langle \tilde{x}' | \mathbf{F}_D \mathbf{Q}^{(\tau)} \mathbf{F}_D^\dagger | \tilde{x} \rangle. \end{aligned}$$

Thus, similarly to conventional random features with Fourier transform (Rahimi & Recht, 2008), if we sampled M features in \mathcal{V}_G from the probability mass function

$$P^{(\tau)}(v_G) := Q^{(\tau)}(v_G) / (\sum_{v'_G \in \mathcal{V}_G} Q^{(\tau)}(v'_G)), \quad (17)$$

corresponding to $d\tau$, we could combine the M features with the discrete Fourier transform \mathbf{F}_D to achieve the learning with kernel $\tilde{k}(\tilde{x}', \tilde{x})$, for sufficiently large M . But $P^{(\tau)}(v_G)$ is not optimized for the data, and we develop a quantum algorithm for sampling an optimized random feature to minimize M .

4.3. Kernels applicable to our quantum algorithm

Our quantum algorithm can use any translation-invariant kernel \tilde{k} given in the form of its perfect reconstruction in Proposition 1, where $Q^{(\tau)}(v_G)$ can be given by any function efficiently computable in a short time denoted by $T'_\tau = O(\text{poly}(D))$. The maximum $Q_{\max}^{(\tau)}$ of $Q^{(\tau)}(v_G)$

$$Q_{\max}^{(\tau)} := \max \{ Q^{(\tau)}(v_G) : v_G \in \mathcal{V}_G \} \quad (18)$$

is also assumed to be given. We assume bounds $\tilde{k}(0, 0) = \Omega(k(0, 0)) = \Omega(1)$ and $Q_{\max}^{(\tau)} = O(\text{poly}(D))$, which mean that the parameters of the kernel function are adjusted appropriately, so that $\tilde{k}(0, 0)$ can reasonably approximate $k(0, 0) = \int_{\mathcal{V}} d\tau(v) = 1$, and $Q_{\max}^{(\tau)} (= \Omega(1))$ may not be too large (e.g. not exponentially large) as D gets large.

We represent computation of $Q^{(\tau)}$ in our algorithm as an oracle \mathcal{O}_τ with runtime $T_\tau = O(T'_\tau)$ per query.⁷ This oracle \mathcal{O}_τ computes $Q^{(\tau)}$ while maintaining the superpositions (i.e. linear combinations) in a given quantum state, that is,

$$\mathcal{O}_\tau \left(\sum_v \alpha_v |v\rangle \otimes |0\rangle \right) = \sum_v \alpha_v |v\rangle \otimes |Q^{(\tau)}(v)\rangle, \quad (19)$$

where $\alpha_v \in \mathbb{C}$ can be any coefficient of a given state, and $|v\rangle$ and $|Q^{(\tau)}(v)\rangle$ are computational-basis states representing bit strings for the fixed-point number representation of $v \in \mathcal{V}$ and $Q^{(\tau)}(v) \in \mathbb{R}$ to sufficient precision.

⁷We can efficiently implement the oracle \mathcal{O}_τ if $Q^{(\tau)}(v_G)$ is computable in a short time T'_τ in classical computation; e.g., if $Q^{(\tau)}(v_G)$ is given in terms of special functions, we can compute it by numerical libraries using arithmetics or lookup tables. If $Q^{(\tau)}$ is computable in time T'_τ by arithmetics, quantum computers can also perform the same arithmetics in time $T_\tau = O(T'_\tau)$ (Häner et al., 2018), and if by a lookup table stored in RAM, quantum computers can instead use the QRAM discussed in Sec. 3.3.

Remark 1. Representative choices of kernels, such as the Gaussian and the Laplacian in Table 3, satisfy our assumptions in a reasonable parameter region. For these kernels, $Q^{(\tau)}$ is a product of D special functions, computable in time $T_\tau = O(T'_\tau) = O(D)$ if each special function is computable in a constant time. It is immediate to give $Q_{\max}^{(\tau)} = Q^{(\tau)}(0)$. We have $\tilde{k}(0, 0) \geq 1 = \Omega(1)$ for these kernels. We can also fulfill $Q_{\max}^{(\tau)} = O(\text{poly}(D))$ by reducing the parameter γ of the kernels in Table 3 as D increases (the reduction of γ enlarges the class of learnable functions). Not only these kernels, we can use any kernel satisfying our assumptions. Our algorithm *does not* impose sparsity or low rank on \mathbf{k} for the kernel and $\hat{\mathbf{q}}^{(\rho)}$ for the data distribution,⁸ and hence is widely applicable compared to existing quantum machine learning algorithms as discussed in Sec. 1.

4.4. Quantum state for optimized random feature

We provide an optimized probability density function $Q_\epsilon^*(v_G)$ for weighting the probability distribution $P^{(\tau)}(v_G)$ on the finite set \mathcal{V}_G of our features, which corresponds to the optimized density $\tilde{q}_\epsilon^*(v)$ for $d\tau$ on the set \mathcal{V} of real-valued features. In place of \tilde{q}_ϵ^* defined as (9), we define

$$Q_\epsilon^*(v_G) \propto \langle \varphi(v_G, \cdot) | \hat{\mathbf{q}}^{(\rho)} (\hat{\Sigma} + \epsilon \mathbb{1})^{-1} | \varphi(v_G, \cdot) \rangle, \quad (20)$$

where the probability distribution $Q_\epsilon^*(v_G) P^{(\tau)}(v_G)$ is normalized by $\sum_{v_G \in \mathcal{V}_G} Q_\epsilon^*(v_G) P^{(\tau)}(v_G) = 1$. To describe a quantum state used for sampling from $Q_\epsilon^*(v_G) P^{(\tau)}(v_G)$, define a full-rank positive semidefinite operator

$$\hat{\Sigma}_\epsilon := (1/Q_{\max}^{(\tau)}) \sqrt{\hat{\mathbf{q}}^{(\rho)}} \mathbf{k} \sqrt{\hat{\mathbf{q}}^{(\rho)}} + (\epsilon/Q_{\max}^{(\tau)}) \mathbb{1}. \quad (21)$$

To establish Algorithm 1, we construct a quantum state for sampling from $Q_\epsilon^*(v_G) P^{(\tau)}(v_G)$ as follows.

Proposition 2 (Quantum state for sampling an optimized random feature). *Define a quantum state*

$$|\Psi\rangle^{XX'} \propto \sum_{\tilde{x} \in \tilde{\mathcal{X}}} \hat{\Sigma}_\epsilon^{-\frac{1}{2}} |\tilde{x}\rangle^X \otimes \sqrt{(1/Q_{\max}^{(\tau)})} \mathbf{Q}^{(\tau)} \mathbf{F}_D^\dagger \sqrt{\hat{\mathbf{q}}^{(\rho)}} |\tilde{x}\rangle^{X'}$$

on two quantum registers $\mathcal{H}^X \otimes \mathcal{H}^{X'}$, where X and X' have the same number of qubits. If we perform a measurement of the quantum register X' on the state $|\Psi\rangle^{XX'}$ in the computational basis $\{|\tilde{x}\rangle^{X'} : \tilde{x} \in \tilde{\mathcal{X}}\}$, we obtain a measurement outcome \tilde{x} with probability $Q_\epsilon^*(\tilde{x}/G) P^{(\tau)}(\tilde{x}/G)$.

4.5. Supervised learning by optimized random features

Given M optimized random features $v_0, \dots, v_{M-1} \in \mathcal{V}_G$ sampled by Algorithm 1 to achieve the learning to accuracy $O(\epsilon)$, we show that we can efficiently perform

⁸The assumption (5) on the upper bound of the degree of freedom $d(\epsilon)$ does not imply low rank of \mathbf{k} and $\hat{\mathbf{q}}^{(\rho)}$ even approximately, while low-rank \mathbf{k} or low-rank $\hat{\mathbf{q}}^{(\rho)}$ would conversely lead to an upper bound of $d(\epsilon)$.

Algorithm 2 Supervised learning by quOptRF.

Input: Inputs to Algorithms 1 and 3, required number M of features for achieving the learning to accuracy $O(\epsilon)$, classical oracles $\mathcal{O}_{\tilde{x}}, \mathcal{O}_y$ in (11).
Output: Optimized random features v_0, \dots, v_{M-1} and coefficients $\alpha_0, \dots, \alpha_{M-1}$ for $\sum_m \alpha_m \varphi(v_m, \cdot)$ to achieve the learning with probability greater than $1 - \delta$.
 1: **for** $m \in \{0, \dots, M-1\}$ **do**
 2: $v_m \leftarrow$ quOptRF. {By Algorithm 1.}
 3: **end for**
 4: Minimize $I(\alpha)$ to accuracy $O(\epsilon)$ by SGD to obtain $\alpha_0, \dots, \alpha_{M-1}$. {By Algorithm 3.}
 5: **Return** $v_0, \dots, v_{M-1}, \alpha_0, \dots, \alpha_{M-1}$.

Algorithm 3 Stochastic gradient descent (SGD).

Input: A function $I : \mathbb{R}^M \rightarrow \mathbb{R}$, a projection Π to a convex parameter region $\mathcal{W} \subset \mathbb{R}^M$, a fixed number of iterations $T \in \mathbb{N}$, an initial point $\alpha^{(1)} \in \mathcal{W}$, T -dependent hyperparameters representing step sizes $(\eta^{(t)} : t = 1, \dots, T)$ given by Jain et al. (2019).
Output: Approximate solution α minimizing $I(\alpha)$.
 1: **for** $t \in \{1, \dots, T\}$ **do**
 2: Calculate $\hat{g}^{(t)}$ satisfying $\mathbb{E}[\hat{g}^{(t)}] = \nabla I(\alpha^{(t)})$.
 3: $\alpha^{(t+1)} \leftarrow \Pi(\alpha^{(t)} - \eta^{(t)} \hat{g}^{(t)})$.
 4: **end for**
 5: **Return** $\alpha \leftarrow \alpha^{(T+1)}$.

linear regression by a classical algorithm to obtain coefficients $\alpha = (\alpha_0, \dots, \alpha_{M-1})^T \in \mathbb{R}^M$ for learning $\sum_{m=0}^{M-1} \alpha_m \varphi(v_m, \cdot) \approx f$. The whole algorithm for achieving the learning is shown in Algorithm 2. As discussed in Sec. 3, we aim to clarify the runtime of the learning in the large-scale limit. The optimal coefficient α minimizes the generalization error

$$I(\alpha) := \sum_{\tilde{x} \in \tilde{\mathcal{X}}} p^{(\rho)}(\tilde{x}) \left| f(\tilde{x}) - \sum_{m=0}^{M-1} \alpha_m \varphi(v_m, \tilde{x}) \right|^2. \quad (22)$$

where the data are IID sampled from $p^{(\rho)}(\tilde{x}) := \int_{\Delta_{\tilde{x}}} d\rho(x)$.

We use stochastic gradient descent (SGD) shown in Algorithm 3 (Jain et al., 2019) for the regression to obtain α minimizing I , as in common practice of large-scale machine learning. The performance of SGD with random features is extensively studied by Carratino et al. (2018), but our contribution is to clarify its *runtime* by explicitly evaluating the runtime per iteration of SGD. We assume sufficiently large number N of data are given; in particular, $N > T$ where T is the number of iterations in the SGD. Then, the sequence of given data $(\tilde{x}_0, y_0), (\tilde{x}_1, y_1), \dots$ provides observations of an IID random variable as assumed in Sec. 3.2, and SGD

converges to the minimum of the generalization error I .⁹

To bound the runtime of the SGD, we show that Algorithm 3 after $O((1/(\epsilon^2 Q_{\min}^2)) \log(1/\delta))$ iterations returns α minimizing I to accuracy ϵ with high probability greater than $1 - \delta$ (Jain et al., 2019), where Q_{\min} is the minimum of $Q(v_0), \dots, Q(v_{M-1})$ in Theorem 1, and the parameter region \mathcal{W} of α in Algorithm 3 is chosen as an M -dimensional ball of center 0 and of radius $O(1/\sqrt{MQ_{\min}})$.¹⁰ In the t th iteration of the SGD for each $t \in \{1, \dots, T\}$, we calculate an (unbiased) estimate $\hat{g}^{(t)}$ of the gradient ∇I . Using the t th IID sampled data (\tilde{x}_t, y_t) and an integer $m \in \{0, \dots, M-1\}$ sampled uniformly, we calculate $\hat{g}^{(t)}$ within time $O(MD)$ in addition to one query to each of the classical oracles $\mathcal{O}_{\tilde{x}}$ and \mathcal{O}_y to get (\tilde{x}_t, y_t) in time $T_{\tilde{x}}$ and T_y , respectively; that is, the runtime per iteration of the SGD is $O(MD + T_{\tilde{x}} + T_y)$. Combining Algorithm 1 with this SGD, we achieve the learning by Algorithm 2 within the following overall runtime.

Theorem 2 (Overall runtime of supervised learning by optimized random features). *The runtime of Algorithm 2 is*

$$O(MT_1) + O((MD + T_{\tilde{x}} + T_y)(1/(\epsilon^2 Q_{\min}^2)) \log(1/\delta)),$$

where T_1 appears in Theorem 1, the first term is the runtime of sampling M optimized random features by Algorithm 1, and the second term is runtime of the SGD. In particular, this runtime is as fast as linear in M and D , i.e. $O(MD)$.

Remark 2. Since our algorithm uses the optimized random features, the required number M of features is expected to be nearly minimal, while it has been computationally hard in practice to use these features in classical computation.

5. Conclusion

We have constructed a quantum algorithm for sampling an *optimized random feature* within a linear time $O(D)$ in data dimension D , achieving an exponential speedup in D compared to the existing classical algorithm of Bach (2017) for this sampling task. Combining M features sampled by this quantum algorithm with stochastic gradient descent, we can achieve supervised learning in time $O(MD)$, where this M is expected to be nearly minimal since we use the optimized random features. As for future work, it is open to prove hardness of sampling an optimized random feature for *any* possible classical algorithm under complexity-theoretical assumptions. It is also interesting to investigate whether

⁹Rather than least-squares of I , Bach (2017) analyzes regularized least-squares regression exploiting Q_ϵ^* , but Q_ϵ^* is hard to compute. We may replace this regularization with L_2 regularization $R(\alpha) = \lambda \|\alpha\|_2^2$. SGD minimizing $I + R$ needs $O(1/(\epsilon\lambda))$ iterations due to strong convexity (Jain et al., 2019), while further research is needed to clarify how this affects the learning accuracy.

¹⁰If important features minimizing M have been sampled, their weight Q_{\min} is expected to be large, not dominating the runtime.

we can reduce the runtime to $O(M \log D)$, as in [Le et al. \(2013\)](#); [Yu et al. \(2016\)](#) but using the optimized random features to achieve minimal M . Since our quantum algorithm does not impose sparsity or low-rank assumptions, our results open a route to a widely applicable framework of kernel-based quantum machine learning with an exponential speedup.

Acknowledgments

This work was supported by CREST (Japan Science and Technology Agency) JPMJCR1671, Cross-ministerial Strategic Innovation Promotion Program (SIP) (Council for Science, Technology and Innovation (CSTI)), a Cambridge-India Ramanujan scholarship from the Cambridge Trust, the SERB (Govt. of India), and JSPS KAKENHI 18K18113.

Supplementary Materials: Fast Quantum Algorithm for Learning with Optimized Random Features

In Supplementary Materials, we summarize basic notions of quantum computation and provide proofs of theorems and propositions in the main text. In Sec. A, the basic notions of quantum computation are summarized. The proofs of Proposition 1, Proposition 2, Theorem 1, and Theorem 2 in the main text are given in Sec. B, Sec. C, Sec. D, and Sec. E, respectively. Note that lemmas that we show for the runtime analysis of our quantum algorithm are presented in Sec. D, and the proofs in the other sections do not require these lemmas on quantum computation.

A. Quantum computation

We summarize basic notions of quantum computation, referring to Nielsen & Chuang (2011); de Wolf (2019) for more detail.

Analogously to a bit $\{0, 1\}$ in classical computation, the unit of quantum computation is a quantum bit (qubit), mathematically represented by \mathbb{C}^2 , i.e., a 2-dimensional complex Hilbert space. A fixed orthonormal basis of a qubit \mathbb{C}^2 is denoted by $\{|0\rangle := \begin{pmatrix} 1 \\ 0 \end{pmatrix}, |1\rangle := \begin{pmatrix} 0 \\ 1 \end{pmatrix}\}$. Similarly to a bit taking a state $b \in \{0, 1\}$, a qubit takes a quantum state $|\psi\rangle = \alpha_0 |0\rangle + \alpha_1 |1\rangle = \begin{pmatrix} \alpha_0 \\ \alpha_1 \end{pmatrix} \in \mathbb{C}^2$. While a register of m bits takes values in $\{0, 1\}^m$, a quantum register of m qubits is represented by the tensor-product space $(\mathbb{C}^2)^{\otimes m} \cong \mathbb{C}^{2^m}$, i.e., a 2^m -dimensional Hilbert space. We may use $=$ rather than \cong to represent isomorphism for brevity. We let \mathcal{H} denote a finite-dimensional Hilbert space representing a quantum register; that is, an m -qubit register is $\mathcal{H} = \mathbb{C}^{2^m}$. A fixed orthonormal basis $\{|x\rangle : x \in \{0, \dots, 2^m - 1\}\}$ of a quantum register \mathcal{H} is called the *computational basis*. A state of \mathcal{H} can be denoted by $|\psi\rangle = \sum_{x=0}^{2^m-1} \alpha_x |x\rangle \in \mathcal{H}$. Note that any quantum state $|\psi\rangle$ requires an L_2 normalization condition $\| |\psi\rangle \|_2 = 1$, and for any $\theta \in \mathbb{R}$, $|\psi\rangle$ is identified with $e^{i\theta} |\psi\rangle$. A conjugate transpose of the column vector $|\psi\rangle$ is a row vector denoted by $\langle \psi |$. The inner product of $|\psi\rangle$ and $|\phi\rangle$ is denoted by $\langle \psi | \phi \rangle$, while their outer product $|\psi\rangle \langle \phi |$ is a matrix. The conjugate transpose of an operator \mathbf{A} is denoted by \mathbf{A}^\dagger , and the transpose of \mathbf{A} with respect to the computational basis is denoted by \mathbf{A}^T .

A measurement of a quantum state $|\psi\rangle$ is a sampling process that returns a randomly chosen bit string from the quantum state. An m -qubit state $|\psi\rangle = \sum_{x=0}^{2^m-1} \alpha_x |x\rangle$ is said to be in a superposition of the basis states $|x\rangle$ s. A measurement of $|\psi\rangle$ in the computational basis $\{|x\rangle\}$ provides a random m -bit string $x \in \{0, 1\}^m$ as outcome, with probability $p(x) = |\alpha_x|^2$. After the measurement, the state changes from $|\psi\rangle$ to $|x\rangle$ corresponding to the obtained outcome x , and loses the randomness in $|\psi\rangle$; that is, to repeat the same sampling as this measurement, we need to prepare $|\psi\rangle$ for each repetition. For two registers $\mathcal{H}^A \otimes \mathcal{H}^B$ and their state $|\phi\rangle^{AB} = \sum_{x,x'} \alpha_{x,x'} |x\rangle^A \otimes |x'\rangle^B \in \mathcal{H}^A \otimes \mathcal{H}^B$, a measurement of the register B for $|\phi\rangle^{AB}$ in the computational basis $\{|x'\rangle^B\}$ of \mathcal{H}^B yields an outcome x' with probability $p(x') = \sum_x p(x, x')$, where $p(x, x') = |\alpha_{x,x'}|^2$. The superscripts of a state or an operator represent which register the state or the operator belongs to, while we may omit the superscripts if it is clear from the context.

A quantum algorithm start by initializing m qubits in a fixed state $|0\rangle^{\otimes m}$, which we may write as $|0\rangle$ if m is clear from the context. Then, we apply a 2^m -dimensional unitary operator \mathbf{U} to $|0\rangle^{\otimes m}$, to prepare a state $\mathbf{U} |0\rangle^{\otimes m}$. Finally, a measurement of $\mathbf{U} |0\rangle^{\otimes m}$ is performed to sample an m -bit string from a probability distribution given by $\mathbf{U} |0\rangle^{\otimes m}$. Analogously to classical logic-gate circuits, \mathbf{U} is represented by a quantum circuit composed of sequential applications of unitaries acting at most two qubits at a time. Each of these unitaries is called an elementary quantum gate. The runtime of a quantum algorithm represented by a quantum circuit is determined by the number of applications of elementary quantum gates in the circuit.

To apply a non-unitary operator \mathbf{A} in quantum computation, we use a *block encoding* (Gilyén et al., 2019). A block encoding of \mathbf{A} is a unitary operator $\mathbf{U} = \begin{pmatrix} \mathbf{A} & \\ & \end{pmatrix}$ that encodes \mathbf{A} in its left-top (or $|0\rangle \langle 0|$) subspace (up to numerical precision). Note that we have

$$\mathbf{U} = \begin{pmatrix} \mathbf{A} & \mathbf{B} \\ & \mathbf{D} \end{pmatrix} = |0\rangle \langle 0| \otimes \mathbf{A} + |0\rangle \langle 1| \otimes \mathbf{B} + |1\rangle \langle 0| \otimes \mathbf{C} + |1\rangle \langle 1| \otimes \mathbf{D}, \quad (23)$$

if \mathbf{A} , \mathbf{B} , \mathbf{C} , and \mathbf{D} are on the Hilbert space of the same dimension. Consider a state $|0\rangle \otimes |\psi\rangle = \begin{pmatrix} |\psi\rangle \\ 0 \end{pmatrix}$ in the top-left (or

$|0\rangle\langle 0|$ subspace of \mathbf{U} , where $\mathbf{0}$ is a zero column vector, and $|0\rangle \in \mathbb{C}^d$ for some d . Applying \mathbf{U} to the state $|0\rangle \otimes |\psi\rangle$, we obtain

$$\mathbf{U}(|0\rangle \otimes |\psi\rangle) = \sqrt{p}|0\rangle \otimes \frac{\mathbf{A}|\psi\rangle}{\|\mathbf{A}|\psi\rangle\|_2} + \sqrt{1-p}|\perp\rangle, \quad (24)$$

where $p = \|\mathbf{A}|\psi\rangle\|_2^2$, and $|\perp\rangle$ is a state satisfying $(|0\rangle\langle 0| \otimes \mathbb{1})|\perp\rangle = 0$ and is of no interest. Then, we can prepare the state $\frac{\mathbf{A}|\psi\rangle}{\|\mathbf{A}|\psi\rangle\|_2}$ using this process for preparing $\mathbf{U}(|0\rangle \otimes |\psi\rangle)$ and its inverse process repeatedly $O(\frac{1}{\sqrt{p}})$ times, by means of amplitude amplification (Brassard et al., 2002). Note that given a quantum circuit, its inverse can be implemented by replacing each gate in the circuit with its inverse gate. In Sec. D, we will use the following more precise definition of block encoding for clarity. For any operator \mathbf{A} on s qubits, i.e., on \mathbb{C}^{2^s} , a unitary operator \mathbf{U} on $(s+a)$ qubits, i.e., on $\mathbb{C}^{2^{s+a}}$, is called an (α, a, Δ) -block encoding of \mathbf{A} if it holds that

$$\left\| \mathbf{A} - \alpha \left(\mathbb{1} \otimes |0\rangle\langle 0|^{\otimes a} \right) \mathbf{U} \left(\mathbb{1} \otimes |0\rangle\langle 0|^{\otimes a} \right) \right\|_{\infty} \leq \Delta, \quad (25)$$

where $\|\cdot\|_{\infty}$ is the operator norm. Note that the discussion on precision Δ is omitted in the main text for simplicity of the presentation. Since any unitary operator \mathbf{U} satisfies $\|\mathbf{U}\|_{\infty} \leq 1$, it is necessary that $\|\mathbf{A}\|_{\infty} \leq \alpha + \Delta$.

B. Proof of Proposition 1

We prove Proposition 1 in the main text on the perfect reconstruction of a translation-invariant kernel.

Proof of Proposition 1. To show the perfect reconstruction of the kernel \tilde{k} , we use the assumption given in the main text that the data domain is finite due to the discretized representation

$$\tilde{\mathcal{X}} = \{0, 1, \dots, G-1\}. \quad (26)$$

As summarized in Sec. 2 in the main text, recall that any translation-invariant kernel $k : \mathcal{X} \times \mathcal{X} \rightarrow \mathbb{R}$ can be written as

$$k(x', x) = k_{\text{TI}}(x' - x) = \int_{\mathcal{V}} d\tau(v) \overline{\varphi(v, x')} \varphi(v, x), \quad (27)$$

where $\varphi(v, x) := e^{-2\pi i v \cdot x}$, and

$$d\tau(v) = q^{(\tau)}(v)dv = \left[\int_{\mathcal{X}} dx e^{-2\pi i v \cdot x} k_{\text{TI}}(x) \right] dv \quad (28)$$

is given by the Fourier transform of the kernel. Also recall that we approximate $k(x', x)$ by

$$\tilde{k}(x', x) = \sum_{n \in \mathbb{Z}^D} k(x', x + Gn). \quad (29)$$

In the same way as k_{TI} , we write

$$\tilde{k}(x', x) = \tilde{k}_{\text{TI}}(x' - x). \quad (30)$$

The function \tilde{k} is periodic; in particular, we have for any $n' \in \mathbb{Z}^D$

$$\tilde{k}(x', x) = \sum_{n \in \mathbb{Z}^D} k(x', x + Gn) = \tilde{k}(x' + Gn', x) = \tilde{k}(x', x + Gn') = \tilde{k}_{\text{TI}}(x' - x + Gn'). \quad (31)$$

Shannon's sampling theorem (Shannon, 1949) in signal processing (Proakis, 2001) shows in the case of $D = 1$ that we can perfectly reconstruct the kernel function \tilde{k}_{TI} on a *continuous* domain $[-\frac{G}{2}, \frac{G}{2}]$ from *discrete* frequencies of its Fourier transform. In the one-dimensional case, the Fourier transform of \tilde{k}_{TI} on $[-\frac{G}{2}, \frac{G}{2}]$ is

$$\int_{-\frac{G}{2}}^{\frac{G}{2}} dx \tilde{k}_{\text{TI}}(x) e^{-2\pi i v x} = \int_{-\infty}^{\infty} dx k_{\text{TI}}(x) e^{-2\pi i v x} = q^{(\tau)}(v). \quad (32)$$

Then, for any $x \in [-\frac{G}{2}, \frac{G}{2}]$, using the discrete frequencies $\tilde{v} \in \mathbb{Z}$ for $q^{(\tau)}(\tilde{v})$, we exactly obtain from the sampling theorem

$$\tilde{k}_{\text{TI}}(x) = \frac{1}{G} \sum_{\tilde{v}=-\infty}^{\infty} q^{(\tau)}\left(\frac{\tilde{v}}{G}\right) e^{2\pi i\left(\frac{\tilde{v}}{G}\right)x} = \frac{1}{G} \sum_{\tilde{v}=-\infty}^{\infty} q^{(\tau)}\left(\frac{\tilde{v}}{G}\right) e^{\frac{2\pi i\tilde{v}x}{G}}. \quad (33)$$

Due to the periodicity (31) of \tilde{k}_{TI} , this equality actually holds for any $x \in \mathbb{R}$. In the same way, for any $D \geq 1$, we have for any $x \in \mathbb{R}^D$

$$\tilde{k}_{\text{TI}}(x) = \frac{1}{G^D} \sum_{\tilde{v} \in \mathbb{Z}^D} q^{(\tau)}\left(\frac{\tilde{v}}{G}\right) e^{\frac{2\pi i\tilde{v} \cdot x}{G}}. \quad (34)$$

In addition, since $\tilde{\mathcal{X}}$ is a *discrete* domain spaced at intervals 1, we can achieve the perfect reconstruction of the kernel \tilde{k}_{TI} on $\tilde{\mathcal{X}}$ by the D -dimensional discrete Fourier transform of \tilde{k}_{TI} , using a *finite* set of discrete frequencies for $q^{(\tau)}$. In particular, for each $\tilde{v} \in \tilde{\mathcal{X}}$, the discrete Fourier transform of \tilde{k}_{TI} yields

$$\begin{aligned} \frac{1}{\sqrt{G^D}} \sum_{\tilde{x} \in \tilde{\mathcal{X}}} \tilde{k}_{\text{TI}}(\tilde{x}) e^{-\frac{2\pi i\tilde{v} \cdot \tilde{x}}{G}} &= \frac{1}{\sqrt{G^D}} \sum_{\tilde{x} \in \tilde{\mathcal{X}}} \left(\frac{1}{G^D} \sum_{\tilde{v}'' \in \mathbb{Z}^D} q^{(\tau)}\left(\frac{\tilde{v}''}{G}\right) e^{\frac{2\pi i\tilde{v}'' \cdot \tilde{x}}{G}} \right) e^{-\frac{2\pi i\tilde{v} \cdot \tilde{x}}{G}} \\ &= \frac{1}{\sqrt{G^D}} \sum_{\tilde{v}' \in \mathbb{Z}^D} q^{(\tau)}\left(\frac{\tilde{v}}{G} + \tilde{v}'\right), \end{aligned} \quad (35)$$

where the sum over \tilde{x} in the first line is nonzero if $\tilde{v}'' = \tilde{v} + G\tilde{v}'$ for any $\tilde{v}' \in \mathbb{Z}^D$. Thus for the perfect reconstruction of the kernel \tilde{k} on this domain $\tilde{\mathcal{X}}$, it suffices to use feature points $v_G = \frac{\tilde{v}}{G}$ for each $\tilde{v} \in \tilde{\mathcal{X}}$, which yields a finite set \mathcal{V}_G of features

$$v_G = \begin{pmatrix} v_G^{(1)} \\ \vdots \\ v_G^{(D)} \end{pmatrix} \in \mathcal{V}_G := \left\{ 0, \frac{1}{G}, \dots, 1 - \frac{1}{G} \right\}^D. \quad (36)$$

We use the one-to-one correspondence between $v_G \in \mathcal{V}_G$ and $\tilde{x} \in \tilde{\mathcal{X}}$ satisfying

$$v_G = \frac{\tilde{x}}{G}, \quad (37)$$

which we may also write using $\tilde{v} = \tilde{x}$ as

$$v_G = \frac{\tilde{v}}{G}. \quad (38)$$

In the same way as the main text, we let $Q^{(\tau)} : \mathcal{V}_G \rightarrow \mathbb{R}$ denote the function in (35)

$$Q^{(\tau)}(v_G) := \sum_{\tilde{v}' \in \mathbb{Z}^D} q^{(\tau)}(v_G + \tilde{v}'). \quad (39)$$

Therefore, from the D -dimensional discrete Fourier transform of (35), we obtain the perfect reconstruction of the kernel \tilde{k}_{TI} on the domain $\tilde{\mathcal{X}}$ using the feature points in \mathcal{V}_G and the function $Q^{(\tau)}$ as

$$\begin{aligned} \tilde{k}(\tilde{x}', \tilde{x}) &= \tilde{k}_{\text{TI}}(\tilde{x}' - \tilde{x}) \\ &= \frac{1}{\sqrt{G^D}} \sum_{\tilde{v} \in \tilde{\mathcal{X}}} \left(\frac{1}{\sqrt{G^D}} \sum_{\tilde{v}' \in \mathbb{Z}^D} q^{(\tau)}\left(\frac{\tilde{v}}{G} + \tilde{v}'\right) \right) e^{\frac{2\pi i\tilde{v} \cdot (\tilde{x}' - \tilde{x})}{G}} = \sum_{v_G \in \mathcal{V}_G} \frac{Q^{(\tau)}(v_G)}{G^D} \overline{\varphi(v_G, \tilde{x}')} \varphi(v_G, \tilde{x}), \quad \forall \tilde{x}', \tilde{x} \in \tilde{\mathcal{X}}, \end{aligned} \quad (40)$$

which shows the first equality in Proposition 1. This equality also has implications discussed in Remark 3 after this proof.

To show the second equality in Proposition (1), we introduce the following notations. We write a diagonal operator corresponding to $Q^{(\tau)}(v_G)$ as

$$\mathbf{Q}^{(\tau)} := \sum_{\tilde{v} \in \tilde{\mathcal{X}}} Q^{(\tau)}\left(\frac{\tilde{v}}{G}\right) |\tilde{v}\rangle \langle \tilde{v}|. \quad (41)$$

Note that we write $|\tilde{v}\rangle = |\tilde{x}\rangle$ for $\tilde{v} = \tilde{x} \in \tilde{\mathcal{X}}$ for clarity of the presentation. In addition, let \mathbf{F} denote a unitary operator representing (one-dimensional) discrete Fourier transform

$$\mathbf{F} := \sum_{\tilde{x}=0}^{G-1} \left(\frac{1}{\sqrt{G}} \sum_{\tilde{v}=0}^{G-1} e^{-\frac{2\pi i \tilde{v} \tilde{x}}{G}} |\tilde{v}\rangle \right) \langle \tilde{x}|, \quad (42)$$

and \mathbf{F}_D denote a unitary operator representing D -dimensional discrete Fourier transform

$$\mathbf{F}_D := \mathbf{F}^{\otimes D} = \sum_{\tilde{x} \in \tilde{\mathcal{X}}} \left(\frac{1}{\sqrt{G^D}} \sum_{\tilde{v} \in \tilde{\mathcal{X}}} e^{-\frac{2\pi i \tilde{v} \cdot \tilde{x}}{G}} |\tilde{v}\rangle \right) \langle \tilde{x}|. \quad (43)$$

The feature map can be written in terms of \mathbf{F}_D as

$$\varphi(v_G, \tilde{x}) = e^{-2\pi i v_G \cdot \tilde{x}} = \sqrt{G^D} \langle \tilde{v} | \mathbf{F}_D | \tilde{x} \rangle = \sqrt{G^D} \langle \tilde{x} | \mathbf{F}_D | \tilde{v} \rangle, \quad (44)$$

where $v_G = \frac{\tilde{v}}{G}$, and the last equality follows from the invariance of \mathbf{F}_D under the transpose with respect to the computational basis. From (40), (43), and (44), by linear algebraic calculation, we obtain for any $\tilde{x}', \tilde{x} \in \tilde{\mathcal{X}}$

$$\tilde{k}(\tilde{x}', \tilde{x}) = \langle \tilde{x}' | \mathbf{F}_D^\dagger \mathbf{Q}^{(\tau)} \mathbf{F}_D | \tilde{x} \rangle = \langle \tilde{x}' | \mathbf{F}_D \mathbf{Q}^{(\tau)} \mathbf{F}_D^\dagger | \tilde{x} \rangle, \quad (45)$$

where the last equality follows from the fact that the kernel function \tilde{k} is symmetric and real, i.e., $\tilde{k}(x', x) = \tilde{k}(x, x')$ and $\overline{\tilde{k}(x', x)} = \tilde{k}(x', x)$. \square

Remark 3. Equality (40) has the following implications. As shown in the main text, we let $P^{(\tau)}$ denote a probability mass function on \mathcal{V}_G proportional to $Q^{(\tau)}$

$$P^{(\tau)}(v_G) := \frac{Q^{(\tau)}(v_G)}{\sum_{v'_G \in \mathcal{V}_G} Q^{(\tau)}(v'_G)}, \quad (46)$$

which by definition satisfies the normalization condition

$$\sum_{v_G \in \mathcal{V}_G} P^{(\tau)}(v_G) = 1. \quad (47)$$

We obtain from (40)

$$\tilde{k}(0, 0) = \sum_{v_G \in \mathcal{V}_G} \frac{Q^{(\tau)}(v_G)}{G^D}, \quad (48)$$

and hence, we can regard $\tilde{k}(0, 0)$ as a normalization factor in

$$P^{(\tau)}(v_G) = \frac{1}{\tilde{k}(0, 0)} \frac{Q^{(\tau)}(v_G)}{G^D}. \quad (49)$$

We also write the maximum of $Q^{(\tau)}(v_G)$ as

$$Q_{\max}^{(\tau)} = \max \left\{ Q^{(\tau)}(v_G) : v_G \in \mathcal{V}_G \right\}. \quad (50)$$

The normalization $P^{(\tau)}$ yields a lower bound of $Q_{\max}^{(\tau)}$

$$Q_{\max}^{(\tau)} = G^D \times \frac{Q_{\max}^{(\tau)}}{G^D} \geq \sum_{v_G \in \mathcal{V}_G} \frac{Q^{(\tau)}(v_G)}{G^D} = \tilde{k}(0, 0) \sum_{v_G \in \mathcal{V}_G} P^{(\tau)}(v_G) = \tilde{k}(0, 0) = \Omega(1), \quad (51)$$

where we use the assumption $\tilde{k}(0, 0) = \Omega(k(0, 0)) = \Omega(1)$.

C. Proof of Proposition 2

We prove Proposition 2 in the main text showing a quantum state for sampling an optimized random feature.

Proof of Proposition 2. The proof is given by linear algebraic calculation. Note that the normalization $\|\Psi\|_2 = 1$ of a quantum state always yields the normalization $\sum_{\tilde{x}' \in \tilde{\mathcal{X}}} p(\tilde{x}') = 1$ of a probability distribution obtained from the measurement of $\mathcal{H}^{X'}$ in the computational basis $\{|\tilde{x}'\rangle^{X'}\}$, and hence we may omit the normalization constant in the following calculation for simplicity of the presentation.

Recall the definition of the optimized probability distribution $Q_\epsilon^*(v_G) P^{(\tau)}(v_G)$

$$Q_\epsilon^*(v_G) P^{(\tau)}(v_G) = \frac{\left\langle \varphi(v_G, \cdot) \left| \hat{\mathbf{q}}^{(\rho)} (\hat{\Sigma} + \epsilon \mathbb{1})^{-1} \right| \varphi(v_G, \cdot) \right\rangle Q^{(\tau)}(v_G)}{\sum_{v'_G \in \mathcal{V}_G} \left\langle \varphi(v'_G, \cdot) \left| \hat{\mathbf{q}}^{(\rho)} (\hat{\Sigma} + \epsilon \mathbb{1})^{-1} \right| \varphi(v'_G, \cdot) \right\rangle Q^{(\tau)}(v'_G)}, \quad (52)$$

where we write

$$\hat{\Sigma} = \mathbf{k} \hat{\mathbf{q}}^{(\rho)}, \quad (53)$$

$$\mathbf{k} = \sum_{\tilde{x}', \tilde{x} \in \tilde{\mathcal{X}}} \tilde{k}(\tilde{x}', \tilde{x}) |\tilde{x}'\rangle \langle \tilde{x}|, \quad (54)$$

$$\hat{\mathbf{q}}^{(\rho)} = \sum_{\tilde{x} \in \tilde{\mathcal{X}}} \hat{q}^{(\rho)}(\tilde{x}) |\tilde{x}\rangle \langle \tilde{x}|. \quad (55)$$

For $v_G = \frac{\tilde{x}}{G}$, it follows from (44) that

$$|\varphi(v_G, \cdot)\rangle = \sqrt{G^D} \mathbf{F}_D |\tilde{x}\rangle. \quad (56)$$

Then, we have

$$\begin{aligned} (52) &= \frac{\left\langle \varphi(v_G, \cdot) \left| \hat{\mathbf{q}}^{(\rho)} (\hat{\Sigma} + \epsilon \mathbb{1})^{-1} \right| \varphi(v_G, \cdot) \right\rangle Q^{(\tau)}(v_G)}{\sum_{v'_G \in \mathcal{V}_G} \frac{Q^{(\tau)}(v'_G)}{G^D} \left\langle \varphi(v'_G, \cdot) \left| \hat{\mathbf{q}}^{(\rho)} (\hat{\Sigma} + \epsilon \mathbb{1})^{-1} \right| \varphi(v'_G, \cdot) \right\rangle G^D} \\ &= \frac{\left\langle \tilde{x} \left| \mathbf{F}_D^\dagger \hat{\mathbf{q}}^{(\rho)} (\hat{\Sigma} + \epsilon \mathbb{1})^{-1} \mathbf{F}_D \right| \tilde{x} \right\rangle Q^{(\tau)}\left(\frac{\tilde{x}}{G}\right)}{\sum_{\tilde{x}' \in \tilde{\mathcal{X}}} Q^{(\tau)}\left(\frac{\tilde{x}'}{G}\right) \left\langle \tilde{x}' \left| \mathbf{F}_D^\dagger \hat{\mathbf{q}}^{(\rho)} (\hat{\Sigma} + \epsilon \mathbb{1})^{-1} \mathbf{F}_D \right| \tilde{x}' \right\rangle} Q^{(\tau)}\left(\frac{\tilde{x}}{G}\right). \end{aligned} \quad (57)$$

Then, using (41) in Sec. B, we obtain

$$(57) = \frac{\left\langle \tilde{x} \left| \sqrt{\mathbf{Q}^{(\tau)}} \mathbf{F}_D^\dagger \hat{\mathbf{q}}^{(\rho)} (\hat{\Sigma} + \epsilon \mathbb{1})^{-1} \mathbf{F}_D \sqrt{\mathbf{Q}^{(\tau)}} \right| \tilde{x} \right\rangle}{\sum_{\tilde{x}' \in \tilde{\mathcal{X}}} \left\langle \tilde{x}' \left| \sqrt{\mathbf{Q}^{(\tau)}} \mathbf{F}_D^\dagger \hat{\mathbf{q}}^{(\rho)} (\hat{\Sigma} + \epsilon \mathbb{1})^{-1} \mathbf{F}_D \sqrt{\mathbf{Q}^{(\tau)}} \right| \tilde{x}' \right\rangle}. \quad (58)$$

Therefore, it holds that

$$\begin{aligned} Q_\epsilon^*\left(\frac{\tilde{x}}{G}\right) P^{(\tau)}\left(\frac{\tilde{x}}{G}\right) &\propto \left\langle \tilde{x} \left| \sqrt{\mathbf{Q}^{(\tau)}} \mathbf{F}_D^\dagger \hat{\mathbf{q}}^{(\rho)} (\hat{\Sigma} + \epsilon \mathbb{1})^{-1} \mathbf{F}_D \sqrt{\mathbf{Q}^{(\tau)}} \right| \tilde{x} \right\rangle \\ &= \left\langle \tilde{x} \left| \sqrt{\frac{1}{Q_{\max}^{(\tau)}} \mathbf{Q}^{(\tau)}} \mathbf{F}_D^\dagger \hat{\mathbf{q}}^{(\rho)} \left(\frac{1}{Q_{\max}^{(\tau)}} \hat{\Sigma} + \frac{\epsilon}{Q_{\max}^{(\tau)}} \mathbb{1} \right)^{-1} \mathbf{F}_D \sqrt{\frac{1}{Q_{\max}^{(\tau)}} \mathbf{Q}^{(\tau)}} \right| \tilde{x} \right\rangle. \end{aligned} \quad (59)$$

To simplify the form of (59), define a positive semidefinite operator on the support of $\mathbf{q}^{(\rho)}$

$$\begin{aligned}\hat{\Sigma}_\epsilon^{(\rho)} &:= \sqrt{\hat{\mathbf{q}}^{(\rho)}} \left(\frac{1}{Q_{\max}^{(\tau)}} \hat{\Sigma} + \frac{\epsilon}{Q_{\max}^{(\tau)}} \mathbb{1} \right) \left(\hat{\mathbf{q}}^{(\rho)} \right)^{-\frac{1}{2}} \\ &= \frac{1}{Q_{\max}^{(\tau)}} \sqrt{\hat{\mathbf{q}}^{(\rho)}} \mathbf{k} \sqrt{\hat{\mathbf{q}}^{(\rho)}} + \frac{\epsilon}{Q_{\max}^{(\tau)}} \Pi^{(\rho)},\end{aligned}\quad (60)$$

where we use $\hat{\Sigma} = \mathbf{k} \hat{\mathbf{q}}^{(\rho)}$, and $\Pi^{(\rho)}$ is a projector onto the support of $\mathbf{q}^{(\rho)}$. In case $\hat{\mathbf{q}}^{(\rho)}$ does not have full rank, $(\hat{\mathbf{q}}^{(\rho)})^{-\frac{1}{2}}$ denotes $\sqrt{(\hat{\mathbf{q}}^{(\rho)})^{-1}}$, where $(\hat{\mathbf{q}}^{(\rho)})^{-1}$ in this case is the Moore-Penrose pseudoinverse of $\hat{\mathbf{q}}^{(\rho)}$. We have by definition

$$\left(\hat{\Sigma}_\epsilon^{(\rho)} \right)^{-1} = \sqrt{\hat{\mathbf{q}}^{(\rho)}} \left(\frac{1}{Q_{\max}^{(\tau)}} \hat{\Sigma} + \frac{\epsilon}{Q_{\max}^{(\tau)}} \mathbb{1} \right)^{-1} \left(\hat{\mathbf{q}}^{(\rho)} \right)^{-\frac{1}{2}}. \quad (61)$$

Correspondingly, in the same way as the main text, we let $\hat{\Sigma}_\epsilon$ denote a positive definite operator that has the full support on \mathcal{H}^X , and coincides with $\hat{\Sigma}_\epsilon^{(\rho)}$ if projected on the support of $\mathbf{q}^{(\rho)}$

$$\hat{\Sigma}_\epsilon := \frac{1}{Q_{\max}^{(\tau)}} \sqrt{\hat{\mathbf{q}}^{(\rho)}} \mathbf{k} \sqrt{\hat{\mathbf{q}}^{(\rho)}} + \frac{\epsilon}{Q_{\max}^{(\tau)}} \mathbb{1}. \quad (62)$$

Note that since $\mathbf{q}^{(\rho)}$ is diagonal and \mathbf{k} is symmetric, we have

$$\hat{\Sigma}_\epsilon = \hat{\Sigma}_\epsilon^T, \quad (63)$$

where the right-hand side represents the transpose with respect to the computational basis. Then, we can rewrite the last line of (59) as

$$\begin{aligned}Q_\epsilon^* \left(\frac{\tilde{x}}{G} \right) P^{(\tau)} \left(\frac{\tilde{x}}{G} \right) &\propto \left\langle \tilde{x} \left| \sqrt{\frac{1}{Q_{\max}^{(\tau)}} \mathbf{Q}^{(\tau)}} \mathbf{F}_D^\dagger \hat{\mathbf{q}}^{(\rho)} \left(\frac{1}{Q_{\max}^{(\tau)}} \hat{\Sigma} + \frac{\epsilon}{Q_{\max}^{(\tau)}} \mathbb{1} \right)^{-1} \mathbf{F}_D \sqrt{\frac{1}{Q_{\max}^{(\tau)}} \mathbf{Q}^{(\tau)}} \right| \tilde{x} \right\rangle \\ &= \left\langle \tilde{x} \left| \sqrt{\frac{1}{Q_{\max}^{(\tau)}} \mathbf{Q}^{(\tau)}} \mathbf{F}_D^\dagger \sqrt{\hat{\mathbf{q}}^{(\rho)}} \left(\hat{\Sigma}_\epsilon^{(\rho)} \right)^{-1} \sqrt{\hat{\mathbf{q}}^{(\rho)}} \mathbf{F}_D \sqrt{\frac{1}{Q_{\max}^{(\tau)}} \mathbf{Q}^{(\tau)}} \right| \tilde{x} \right\rangle \\ &= \left\langle \tilde{x} \left| \sqrt{\frac{1}{Q_{\max}^{(\tau)}} \mathbf{Q}^{(\tau)}} \mathbf{F}_D^\dagger \sqrt{\hat{\mathbf{q}}^{(\rho)}} \hat{\Sigma}_\epsilon^{-1} \sqrt{\hat{\mathbf{q}}^{(\rho)}} \mathbf{F}_D \sqrt{\frac{1}{Q_{\max}^{(\tau)}} \mathbf{Q}^{(\tau)}} \right| \tilde{x} \right\rangle,\end{aligned}\quad (64)$$

where this probability distribution is normalized by $\sum_{\tilde{x} \in \tilde{\mathcal{X}}} Q_\epsilon^* \left(\frac{\tilde{x}}{G} \right) P^{(\tau)} \left(\frac{\tilde{x}}{G} \right) = 1$.

To prove the proposition, we analyze the probability distribution obtained from a measurement of the quantum state

$$|\Psi\rangle^{XX'} \propto \sum_{\tilde{x} \in \tilde{\mathcal{X}}} \hat{\Sigma}_\epsilon^{-\frac{1}{2}} |\tilde{x}\rangle^X \otimes \sqrt{\frac{1}{Q_{\max}^{(\tau)}} \mathbf{Q}^{(\tau)}} \mathbf{F}_D^\dagger \sqrt{\hat{\mathbf{q}}^{(\rho)}} |\tilde{x}\rangle^{X'} \in \mathcal{H}^X \otimes \mathcal{H}^{X'}. \quad (65)$$

For any operators A on \mathcal{H}^X and B on $\mathcal{H}^{X'}$ where the dimensions of these Hilbert spaces are the same

$$\dim \mathcal{H}^X = \dim \mathcal{H}^{X'}, \quad (66)$$

a straightforward linear-algebraic calculation shows (Nielsen & Chuang, 2011)

$$\sum_{\tilde{x} \in \tilde{\mathcal{X}}} A |\tilde{x}\rangle^X \otimes B |\tilde{x}\rangle^{X'} = \sum_{\tilde{x} \in \tilde{\mathcal{X}}} |\tilde{x}\rangle^X \otimes B A^T |\tilde{x}\rangle^{X'}. \quad (67)$$

Applying this equality to (65), we have

$$\begin{aligned}
 |\Psi\rangle^{XX'} &\propto \sum_{\tilde{x} \in \tilde{\mathcal{X}}} \hat{\Sigma}_\epsilon^{-\frac{1}{2}} |\tilde{x}\rangle^X \otimes \sqrt{\frac{1}{Q_{\max}^{(\tau)}}} \mathbf{Q}^{(\tau)} \mathbf{F}_D^\dagger \sqrt{\hat{\mathbf{q}}^{(\rho)}} |\tilde{x}\rangle^{X'} \\
 &= \sum_{\tilde{x} \in \tilde{\mathcal{X}}} |\tilde{x}\rangle^X \otimes \sqrt{\frac{1}{Q_{\max}^{(\tau)}}} \mathbf{Q}^{(\tau)} \mathbf{F}_D^\dagger \sqrt{\hat{\mathbf{q}}^{(\rho)}} \left(\hat{\Sigma}_\epsilon^T\right)^{-\frac{1}{2}} |\tilde{x}\rangle^{X'} \\
 &= \sum_{\tilde{x} \in \tilde{\mathcal{X}}} |\tilde{x}\rangle^X \otimes \sqrt{\frac{1}{Q_{\max}^{(\tau)}}} \mathbf{Q}^{(\tau)} \mathbf{F}_D^\dagger \sqrt{\hat{\mathbf{q}}^{(\rho)}} \hat{\Sigma}_\epsilon^{-\frac{1}{2}} |\tilde{x}\rangle^{X'}, \tag{68}
 \end{aligned}$$

where the last line follows from (63). If we performed a measurement of $|\Psi\rangle^{XX'}$ in the computational basis $\{|\tilde{x}\rangle^X \otimes |\tilde{x}'\rangle^{X'}\}$, the probability distribution of measurement outcomes, i.e., the square of the amplitude as summarized in Sec. A, would be

$$\begin{aligned}
 p(\tilde{x}, \tilde{x}') &= \left| \langle \tilde{x}|^X \otimes \langle \tilde{x}'|^{X'} | \Psi \rangle^{XX'} \right|^2 \\
 &\propto \left| \left\langle \tilde{x}' \left| \sqrt{\frac{1}{Q_{\max}^{(\tau)}}} \mathbf{Q}^{(\tau)} \mathbf{F}_D^\dagger \sqrt{\hat{\mathbf{q}}^{(\rho)}} \hat{\Sigma}_\epsilon^{-\frac{1}{2}} \right| \tilde{x} \right\rangle \right|^2 \\
 &= \left\langle \tilde{x}' \left| \sqrt{\frac{1}{Q_{\max}^{(\tau)}}} \mathbf{Q}^{(\tau)} \mathbf{F}_D^\dagger \sqrt{\hat{\mathbf{q}}^{(\rho)}} \hat{\Sigma}_\epsilon^{-\frac{1}{2}} \right| \tilde{x} \right\rangle \left\langle \tilde{x} \left| \hat{\Sigma}_\epsilon^{-\frac{1}{2}} \sqrt{\hat{\mathbf{q}}^{(\rho)}} \mathbf{F}_D \sqrt{\frac{1}{Q_{\max}^{(\tau)}}} \mathbf{Q}^{(\tau)} \right| \tilde{x}' \right\rangle. \tag{69}
 \end{aligned}$$

Since a measurement of the register X' yields an outcome \tilde{x}' with probability $p(\tilde{x}') = \sum_{\tilde{x} \in \tilde{\mathcal{X}}} p(\tilde{x}, \tilde{x}')$ as summarized in Sec. A, we obtain

$$\begin{aligned}
 p(\tilde{x}') &\propto \sum_{\tilde{x} \in \tilde{\mathcal{X}}} \left\langle \tilde{x}' \left| \sqrt{\frac{1}{Q_{\max}^{(\tau)}}} \mathbf{Q}^{(\tau)} \mathbf{F}_D^\dagger \sqrt{\hat{\mathbf{q}}^{(\rho)}} \hat{\Sigma}_\epsilon^{-\frac{1}{2}} \right| \tilde{x} \right\rangle \left\langle \tilde{x} \left| \hat{\Sigma}_\epsilon^{-\frac{1}{2}} \sqrt{\hat{\mathbf{q}}^{(\rho)}} \mathbf{F}_D \sqrt{\frac{1}{Q_{\max}^{(\tau)}}} \mathbf{Q}^{(\tau)} \right| \tilde{x}' \right\rangle \\
 &= \left\langle \tilde{x}' \left| \sqrt{\frac{1}{Q_{\max}^{(\tau)}}} \mathbf{Q}^{(\tau)} \mathbf{F}_D^\dagger \sqrt{\hat{\mathbf{q}}^{(\rho)}} \hat{\Sigma}_\epsilon^{-\frac{1}{2}} \left(\sum_{\tilde{x} \in \tilde{\mathcal{X}}} |\tilde{x}\rangle \langle \tilde{x}| \right) \hat{\Sigma}_\epsilon^{-\frac{1}{2}} \sqrt{\hat{\mathbf{q}}^{(\rho)}} \mathbf{F}_D \sqrt{\frac{1}{Q_{\max}^{(\tau)}}} \mathbf{Q}^{(\tau)} \right| \tilde{x}' \right\rangle \\
 &= \left\langle \tilde{x}' \left| \sqrt{\frac{1}{Q_{\max}^{(\tau)}}} \mathbf{Q}^{(\tau)} \mathbf{F}_D^\dagger \sqrt{\hat{\mathbf{q}}^{(\rho)}} \hat{\Sigma}_\epsilon^{-\frac{1}{2}} \mathbb{1} \hat{\Sigma}_\epsilon^{-\frac{1}{2}} \sqrt{\hat{\mathbf{q}}^{(\rho)}} \mathbf{F}_D \sqrt{\frac{1}{Q_{\max}^{(\tau)}}} \mathbf{Q}^{(\tau)} \right| \tilde{x}' \right\rangle \\
 &= \left\langle \tilde{x}' \left| \sqrt{\frac{1}{Q_{\max}^{(\tau)}}} \mathbf{Q}^{(\tau)} \mathbf{F}_D^\dagger \sqrt{\hat{\mathbf{q}}^{(\rho)}} \hat{\Sigma}_\epsilon^{-1} \sqrt{\hat{\mathbf{q}}^{(\rho)}} \mathbf{F}_D \sqrt{\frac{1}{Q_{\max}^{(\tau)}}} \mathbf{Q}^{(\tau)} \right| \tilde{x}' \right\rangle. \tag{70}
 \end{aligned}$$

Recall that the normalization $\| |\Psi\rangle^{XX'} \|_2 = 1$ of the quantum state yields $\sum_{\tilde{x}' \in \tilde{\mathcal{X}}} p(\tilde{x}') = 1$. Therefore, (64) and (70) yield

$$p(\tilde{x}) = Q_\epsilon^* \left(\frac{\tilde{x}}{G} \right) P^{(\tau)} \left(\frac{\tilde{x}}{G} \right), \tag{71}$$

which shows the conclusion. \square

D. Proof of Theorem 1

We prove Theorem 1 in the main text on the runtime of Algorithm 1 for sampling an optimized random feature by quantum computation. Note that each line of Algorithm 1 is performed approximately with a sufficiently small precision to achieve the overall sampling precision $\Delta > 0$, in the same way as classical algorithms that deal with real numbers using fixed- or floating-point number representation with a sufficiently small precision.

Algorithm 1 combines two fundamental subroutines of quantum algorithms, namely, quantum Fourier transform (QFT) (Hales & Hallgren, 2000) and quantum singular value transformation (QSVT) (Gilyén et al., 2019). Using

QFT, we can implement the unitary operator \mathbf{F} defined as (42) with precision Δ by a quantum circuit composed of $O\left(\log(G) \log \log(G) \text{polylog}\left(\frac{1}{\Delta}\right)\right)$ gates (Hales & Hallgren, 2000). Thus, we can implement $\mathbf{F}_D = F^{\otimes D}$ defined as (43) by a quantum circuit composed of gates of order

$$O\left(D \log(G) \log \log(G) \text{polylog}\left(\frac{1}{\Delta}\right)\right). \quad (72)$$

In our analysis, we multiply two numbers represented by $O(\log(G))$ bits using the algorithm shown in (Harvey & Van Der Hoeven, 2019) within time

$$O(\log(G) \log \log(G)). \quad (73)$$

Note that we could also use exact quantum Fourier transform (Nielsen & Chuang, 2011) or grammar-school-method multiplication instead of these algorithms in (Hales & Hallgren, 2000; Harvey & Van Der Hoeven, 2019), to decrease a constant factor in the runtime of our algorithm at the expense of logarithmically increasing the asymptotic scaling in terms of G from $\log(G) \log \log(G)$ to $(\log(G))^2$. To prove Theorem 1, in the following, we show efficient constructions of block encodings; in particular, we first show a block encoding of $\sqrt{\frac{1}{Q_{\max}^{(\tau)}} \mathbf{Q}^{(\tau)}}$, and then using this block encoding, we show that of $\hat{\Sigma}_\epsilon$. For clarity, we use the definition (25) of block encoding in Sec. A. Then, we will provide the runtime analysis of Algorithm 1 using these block encodings.

Our construction of block encodings of $\sqrt{\frac{1}{Q_{\max}^{(\tau)}} \mathbf{Q}^{(\tau)}}$ and $\hat{\Sigma}_\epsilon$ is based on a prescription of constructing a block encoding from a quantum circuit for implementing a measurement described by a positive operator-valued measure (POVM) (Gilyén et al., 2019). In particular, for any precision $\Delta > 0$ and any POVM operator \mathbf{A} , that is, an operator satisfying $0 \leq \mathbf{A} \leq \mathbb{1}$, let \mathbf{U} be a unitary operator represented by a quantum circuit that satisfies for any state $|\psi\rangle$

$$\left| \text{Tr} [|\psi\rangle \langle \psi| \mathbf{A}] - \text{Tr} \left[\mathbf{U} \left(|0\rangle \langle 0|^{\otimes n} \otimes |\psi\rangle \langle \psi| \right) \mathbf{U}^\dagger \left(|0\rangle \langle 0|^{\otimes 1} \otimes \mathbb{1} \right) \right] \right| \leq \Delta, \quad (74)$$

where $|0\rangle^{\otimes n}$ is a fixed state of n auxiliary qubits. The term $\text{Tr} \left[\mathbf{U} \left(|0\rangle \langle 0|^{\otimes n} \otimes |\psi\rangle \langle \psi| \right) \mathbf{U}^\dagger \left(|0\rangle \langle 0|^{\otimes 1} \otimes \mathbb{1} \right) \right]$ has the following meaning: given any input state $|\psi\rangle$ and n auxiliary qubits initially prepared in $|0\rangle^{\otimes n}$, if we perform the circuit \mathbf{U} to obtain a state $\mathbf{U} \left(|0\rangle^{\otimes n} \otimes |\psi\rangle \right)$ and perform a measurement of one of the qubits for the obtained state in the computational basis $\{|0\rangle, |1\rangle\}$, then we obtain a measurement outcome 0 with probability

$$\text{Tr} \left[\mathbf{U} \left(|0\rangle \langle 0|^{\otimes n} \otimes |\psi\rangle \langle \psi| \right) \mathbf{U}^\dagger \left(|0\rangle \langle 0|^{\otimes 1} \otimes \mathbb{1} \right) \right]. \quad (75)$$

Then, it is known that we can construct a $(1, 1+n, \Delta)$ -block encoding of \mathbf{A} using one \mathbf{U} , one \mathbf{U}^\dagger , and one quantum logic gate (i.e., the controlled NOT (CNOT) gate) (Gilyén et al., 2019). The CNOT gate is defined as a two-qubit unitary operator

$$\text{CNOT} := |0\rangle \langle 0| \otimes \mathbb{1} + |1\rangle \langle 1| \otimes \sigma_x, \quad (76)$$

where the first qubit is a controlled qubit, the second qubit is a target qubit, and σ_x is a Pauli unitary operator

$$\sigma_x := |0\rangle \langle 1| + |1\rangle \langle 0|. \quad (77)$$

The CNOT gate acts as

$$\text{CNOT}((\alpha_0 |0\rangle + \alpha_1 |1\rangle) \otimes |0\rangle) = \alpha_0 |0\rangle \otimes |0\rangle + \alpha_1 |1\rangle \otimes |1\rangle. \quad (78)$$

Note that for a given POVM operator \mathbf{A} , no general way of constructing the circuit representing \mathbf{U} in (74) has been shown in (Gilyén et al., 2019). In contrast, we here explicitly construct the circuit for a diagonal POVM operator $\mathbf{A} = \sqrt{\frac{1}{Q_{\max}^{(\tau)}} \mathbf{Q}^{(\tau)}}$ in the following lemma, using the quantum oracle \mathcal{O}_τ . Note that since a diagonal operator is sparse, a conventional way of implementing the block encoding of a sparse operator (Gilyén et al., 2019) would also be applicable to construct a block encoding of $\sqrt{\frac{1}{Q_{\max}^{(\tau)}} \mathbf{Q}^{(\tau)}}$, but our key contribution here is to use the circuit for the block encoding of $\sqrt{\frac{1}{Q_{\max}^{(\tau)}} \mathbf{Q}^{(\tau)}}$ as a building block of a more complicated block encoding, i.e., the block encoding of $\hat{\Sigma}_\epsilon$, which is not necessarily sparse or of low rank. Recall the definition of \mathcal{O}_τ

$$\mathcal{O}_\tau \left(\sum_v \alpha_v |v\rangle \otimes |0\rangle \right) = \sum_v \alpha_v |v\rangle \otimes |Q^{(\tau)}(v)\rangle, \quad (79)$$

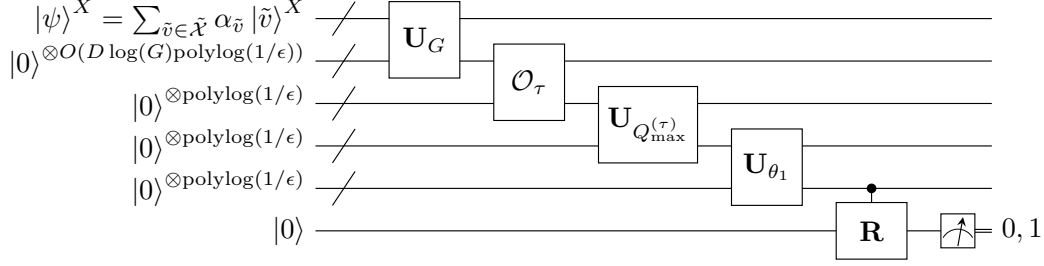


Figure 1. A quantum circuit representing a unitary operator \mathbf{U} that achieves (74) for $\Lambda = \sqrt{\frac{1}{Q_{\max}^{(\tau)}} \mathbf{Q}^{(\tau)}}$, which can be used for implementing a block encoding of $\sqrt{\frac{1}{Q_{\max}^{(\tau)}} \mathbf{Q}^{(\tau)}}$. This circuit achieves the transformation of quantum states shown in a chain starting from (87). The last controlled gate represents \mathbf{CR} . Regarding the notations on quantum circuits, see, e.g., Nielsen & Chuang (2011).

where $\alpha_v \in \mathbb{C}$ can be any coefficient of a given state, and $|v\rangle$ and $|Q^{(\tau)}(v)\rangle$ are computational-basis states representing bit strings for the fixed-point number representation of $v \in \mathcal{V}$ and $Q^{(\tau)}(v) \in \mathbb{R}$ to sufficient precision. In the following of this section, the quantum registers for storing real numbers use fixed-point number representation with sufficient precision $O(\Delta)$ to achieve the overall precision Δ .

Lemma 1 (Block encoding of a diagonal POVM operator). *For any diagonal positive semidefinite operator $\mathbf{Q}^{(\tau)}$ defined as (41), we can implement a $(1, O(D \log(G) \text{polylog}(\frac{1}{\Delta})), \Delta)$ -block encoding of $\sqrt{\frac{1}{Q_{\max}^{(\tau)}} \mathbf{Q}^{(\tau)}}$ by a quantum circuit composed of $O(D \log(G) \log \log(G) \text{polylog}(\frac{1}{\Delta}))$ gates and one query to the quantum oracle \mathcal{O}_τ .*

Proof. We construct a quantum circuit representing a unitary operator \mathbf{U} that achieves (74) for $\Lambda = \sqrt{\frac{1}{Q_{\max}^{(\tau)}} \mathbf{Q}^{(\tau)}}$. We write the input quantum state as

$$|\psi\rangle^X = \sum_{\tilde{v} \in \tilde{\mathcal{X}}} \alpha_{\tilde{v}} |\tilde{v}\rangle^X \in \mathcal{H}^X. \quad (80)$$

Define a function

$$\theta_1(q) := \arccos\left(q^{\frac{1}{4}}\right). \quad (81)$$

Define unitary operators \mathbf{U}_G , $\mathbf{U}_{Q_{\max}^{(\tau)}}$, and \mathbf{U}_{θ_1} acting as

$$\mathbf{U}_G : |x\rangle \otimes |0\rangle \xrightarrow{\mathbf{U}_G} |x\rangle \otimes \left| \frac{x}{G} \right\rangle, \quad (82)$$

$$\mathbf{U}_{Q_{\max}^{(\tau)}} : |x\rangle \otimes |0\rangle \xrightarrow{\mathbf{U}_{Q_{\max}^{(\tau)}}} |x\rangle \otimes \left| \frac{x}{Q_{\max}^{(\tau)}} \right\rangle, \quad (83)$$

$$\mathbf{U}_{\theta_1} : |x\rangle \otimes |0\rangle \xrightarrow{\mathbf{U}_{\theta_1}} |x\rangle \otimes |\theta_1(x)\rangle. \quad (84)$$

Let \mathbf{R}_θ denote a unitary operator representing a one-qubit rotation

$$\mathbf{R}_\theta := \begin{pmatrix} \cos \theta & -\sin \theta \\ \sin \theta & \cos \theta \end{pmatrix}, \quad (85)$$

and a controlled rotation \mathbf{CR} is defined as

$$\mathbf{CR} = \sum_{\theta} |\theta\rangle \langle \theta| \otimes \mathbf{R}_\theta. \quad (86)$$

Using these notations, we show a quantum circuit representing \mathbf{U} in Fig. 1. This circuit achieves the following transformation

up to precision Δ

$$|\psi\rangle \otimes |0\rangle \otimes |0\rangle \otimes |0\rangle \otimes |0\rangle \otimes |0\rangle \quad (87)$$

$$\xrightarrow{U_G} \sum_{\tilde{v}} \alpha_{\tilde{v}} |\tilde{v}\rangle \otimes \left| \frac{\tilde{v}}{G} \right\rangle \otimes |0\rangle \otimes |0\rangle \otimes |0\rangle \otimes |0\rangle \quad (88)$$

$$\xrightarrow{\mathcal{O}_\tau} \sum_{\tilde{v}} \alpha_{\tilde{v}} |\tilde{v}\rangle \otimes \left| \frac{\tilde{v}}{G} \right\rangle \otimes \left| Q^{(\tau)} \left(\frac{\tilde{v}}{G} \right) \right\rangle \otimes |0\rangle \otimes |0\rangle \otimes |0\rangle \quad (89)$$

$$\xrightarrow{U_{Q_{\max}^{(\tau)}}} \sum_{\tilde{v}} \alpha_{\tilde{v}} |\tilde{v}\rangle \otimes \left| \frac{\tilde{v}}{G} \right\rangle \otimes \left| Q^{(\tau)} \left(\frac{\tilde{v}}{G} \right) \right\rangle \otimes \left| \frac{Q^{(\tau)} \left(\frac{\tilde{v}}{G} \right)}{Q_{\max}^{(\tau)}} \right\rangle \otimes |0\rangle \otimes |0\rangle \quad (90)$$

$$\xrightarrow{U_{\theta_1}} \sum_{\tilde{v}} \alpha_{\tilde{v}} |\tilde{v}\rangle \otimes \left| \frac{\tilde{v}}{G} \right\rangle \otimes \left| Q^{(\tau)} \left(\frac{\tilde{v}}{G} \right) \right\rangle \otimes \left| \frac{Q^{(\tau)} \left(\frac{\tilde{v}}{G} \right)}{Q_{\max}^{(\tau)}} \right\rangle \otimes \left| \theta_1 \left(\frac{Q^{(\tau)} \left(\frac{\tilde{v}}{G} \right)}{Q_{\max}^{(\tau)}} \right) \right\rangle \otimes |0\rangle \quad (91)$$

$$\xrightarrow{\mathbf{CR}} \sum_{\tilde{v}} \alpha_{\tilde{v}} |\tilde{v}\rangle \otimes \left| \frac{\tilde{v}}{G} \right\rangle \otimes \left| Q^{(\tau)} \left(\frac{\tilde{v}}{G} \right) \right\rangle \otimes \left| \frac{Q^{(\tau)} \left(\frac{\tilde{v}}{G} \right)}{Q_{\max}^{(\tau)}} \right\rangle \otimes \left| \theta_1 \left(\frac{Q^{(\tau)} \left(\frac{\tilde{v}}{G} \right)}{Q_{\max}^{(\tau)}} \right) \right\rangle \otimes \left(\left(\frac{1}{Q_{\max}^{(\tau)}} Q^{(\tau)} \left(\frac{\tilde{v}}{G} \right) \right)^{\frac{1}{4}} |0\rangle + \sqrt{1 - \sqrt{\frac{1}{Q_{\max}^{(\tau)}} Q^{(\tau)} \left(\frac{\tilde{v}}{G} \right)}} |1\rangle \right), \quad (92)$$

where the quantum registers for storing real numbers use fixed-point number representation with sufficient precision $O(\Delta)$ to achieve the overall precision Δ in (74). In (88), each of the D elements of the vector \tilde{v} in the first quantum register is multiplied by $\frac{1}{G}$ using arithmetics, and the result is stored in the second quantum register. Since $\frac{1}{G}$ can be approximately represented with precision $O(\Delta)$ using $O(\log(\frac{1}{\Delta}))$ bits, these D multiplications take $O(D \log(G) \log \log(G) \text{polylog}(\frac{1}{\Delta}))$ time due to (73), which is dominant. The runtime of the quantum oracle \mathcal{O}_τ queried in (89) is T_τ . We can multiply $\frac{1}{Q_{\max}^{(\tau)}}$ in (90) and calculate the elementary function θ_1 in (91) up to precision $O(\Delta)$ by arithmetics within time $O(\text{polylog}(\frac{1}{\Delta}))$ (Häner et al., 2018). In (92), we apply the controlled \mathbf{R} , i.e., \mathbf{CR} , defined as (86) to the last qubit controlled by the second last quantum register, which uses $O(\text{polylog}(\frac{1}{\Delta}))$ gates since $|\theta\rangle$ stored in the second last register consists of $O(\text{polylog}(\frac{1}{\Delta}))$ qubits. The measurement of the last qubit of (92) in the computational basis $\{|0\rangle, |1\rangle\}$ yields the outcome 0 with probability

$$\sum_{\tilde{v} \in \tilde{\mathcal{X}}} |\alpha_{\tilde{v}}|^2 \sqrt{\frac{1}{Q_{\max}^{(\tau)}} Q^{(\tau)} \left(\frac{\tilde{v}}{G} \right)} = \text{Tr} \left[|\psi\rangle \langle \psi| \sqrt{\frac{1}{Q_{\max}^{(\tau)}} \mathbf{Q}^{(\tau)}} \right], \quad (93)$$

which achieves (74) for $\Lambda = \sqrt{\frac{1}{Q_{\max}^{(\tau)}} \mathbf{Q}^{(\tau)}}$ within the claimed runtime. \square

Using the block encoding of $\sqrt{\frac{1}{Q_{\max}^{(\tau)}} \mathbf{Q}^{(\tau)}}$ as a building block, we construct a block encoding of $\hat{\Sigma}_\epsilon$ in the following. Note that while the following proposition provides a $(1, O(D \log(G) \text{polylog}(\frac{1}{\Delta})), \Delta)$ -block encoding of $\frac{1}{1 + (\epsilon/Q_{\max}^{(\tau)})} \hat{\Sigma}_\epsilon$, this block encoding is equivalently a $(1 + (\epsilon/Q_{\max}^{(\tau)}), O(D \log(G) \text{polylog}(\frac{1}{\Delta})), (1 + (\epsilon/Q_{\max}^{(\tau)})) \Delta)$ -block encoding of $\hat{\Sigma}_\epsilon$ by definition. In implementing the block encoding of $\hat{\Sigma}_\epsilon$, we use the quantum oracle \mathcal{O}_ρ

$$\mathcal{O}_\rho(|0\rangle) = \sum_{\tilde{x} \in \tilde{\mathcal{X}}} \sqrt{\hat{q}^{(\rho)}(\tilde{x})} |\tilde{x}\rangle = \sqrt{\hat{\mathbf{q}}^{(\rho)}} \sum_{\tilde{x} \in \tilde{\mathcal{X}}} |\tilde{x}\rangle. \quad (94)$$

Lemma 2 (Block encoding of $\hat{\Sigma}_\epsilon$). *For any $\epsilon > 0$ and any operator $\hat{\Sigma}_\epsilon$ given in the form of (62), we can implement a $(1, O(D \log(G) \text{polylog}(\frac{1}{\Delta})), \Delta)$ -block encoding of*

$$\frac{1}{1 + (\epsilon/Q_{\max}^{(\tau)})} \hat{\Sigma}_\epsilon$$

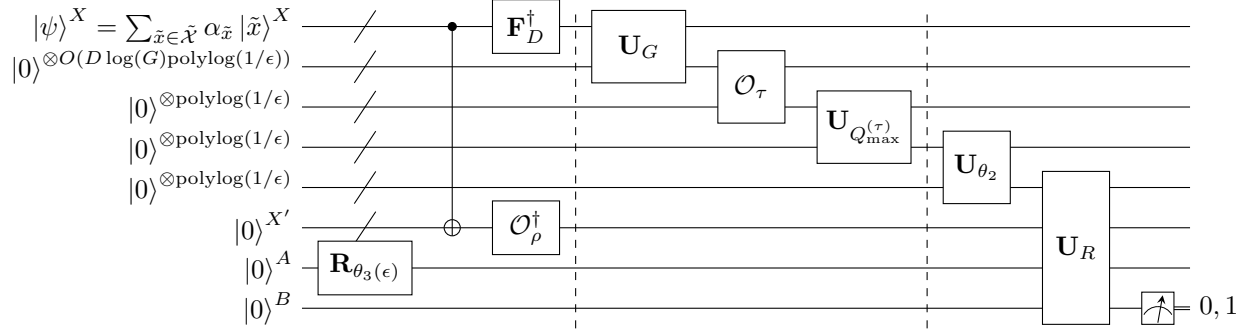


Figure 2. A quantum circuit representing a unitary operator \mathbf{U} that achieves (74) for $\Lambda = \hat{\Sigma}_\epsilon$, which can be used for implementing a block encoding of $\hat{\Sigma}_\epsilon$. The notations are the same as those in Fig. 1. The first gate acting on two quantum registers X and X' collectively represents CNOT gates acting transversally on each of the qubits of these registers. A part of this circuit sandwiched by two vertical dashed lines is the same as the corresponding part in Fig. 1. Additionally, the circuit performs a preprocessing of the input state before performing the part corresponding to Fig. 1, which achieves the transformation of quantum states shown in a chain starting from (100). Also, the circuit performs the final gates \mathbf{U}_{θ_2} and \mathbf{U}_R after the part corresponding to Fig. 1, which are followed by a measurement described by the analysis starting from (103).

by a quantum circuit composed of $O(D \log(G) \log \log(G) \text{polylog}(\frac{1}{\Delta}))$ gates, one query to the quantum oracle \mathcal{O}_ρ^\dagger , i.e., the inverse of \mathcal{O}_ρ , and one query to the quantum oracle \mathcal{O}_τ .

Proof. We construct a quantum circuit representing a unitary operator \mathbf{U} that achieves (74) for $\Lambda = \hat{\Sigma}_\epsilon$. We use the same notations as those in the proof of Lemma 1 except the following notations. The input state is written in this proof as

$$|\psi\rangle^X = \sum_{\tilde{x} \in \tilde{\mathcal{X}}} \alpha_{\tilde{x}} |\tilde{x}\rangle^X \in \mathcal{H}^X. \quad (95)$$

Define functions

$$\theta_2(q) := \arccos(\sqrt{q}), \quad (96)$$

$$\theta_3(\epsilon) := \arccos\left(\sqrt{\frac{\epsilon/Q_{\max}^{(\tau)}}{1 + (\epsilon/Q_{\max}^{(\tau)})}}\right). \quad (97)$$

Define a unitary operator \mathbf{U}_{θ_2} acting as

$$\mathbf{U}_{\theta_2} : |x\rangle \otimes |0\rangle \xrightarrow{U_{\theta_2}} |x\rangle \otimes |\theta_2(x)\rangle. \quad (98)$$

Let \mathbf{U}_ρ denote a unitary operator representing a quantum circuit for implementing the oracle \mathcal{O}_ρ . Then, the unitary operator representing its inverse \mathcal{O}_ρ^\dagger is given by \mathbf{U}_ρ^\dagger . Define a unitary operator

$$\begin{aligned} \mathbf{U}_R = & \left(\mathbb{1} \otimes \mathbb{1}^{X'} \otimes |0\rangle \langle 0|^A \otimes \mathbb{1}^B \right) \\ & + \left(\sum_{\theta} |\theta\rangle \langle \theta| \otimes \left(\mathbb{1}^{X'} - |0\rangle \langle 0|^{X'} \right) \otimes |1\rangle \langle 1|^A \otimes \sigma_x^B \right) + \left(\sum_{\theta} |\theta\rangle \langle \theta| \otimes |0\rangle \langle 0|^{X'} \otimes |1\rangle \langle 1|^A \otimes \mathbf{R}_\theta^B \right), \quad (99) \end{aligned}$$

where the first quantum register may store a real number θ by the fixed-point number representation with sufficient precision to achieve the overall precision Δ in (74), the second quantum register $\mathcal{H}^{X'}$ is isomorphic to the quantum register \mathcal{H}^X , i.e., is composed of the same number of qubits as \mathcal{H}^X , the third quantum register \mathcal{H}^A is one auxiliary qubit, the fourth quantum register \mathcal{H}^B is also one qubit. The operators σ_x^B and \mathbf{R}_θ^B on \mathcal{H}^B are defined as (77) and (85), respectively. Unless the state of X' is $|0\rangle^{X'}$, σ_x^B in the second term flips $|0\rangle^B$ to $|1\rangle^B$, and if the state of X' is $|0\rangle^{X'}$, \mathbf{R}_θ^B in the third term acts in the same way as (92).

Using these notations, we show a quantum circuit representing \mathbf{U} in Fig. 2. While a part of the circuit in Fig. 2 sandwiched by two vertical dashed lines is the same as the corresponding part in Fig. 1, this circuit additionally performs a preprocessing of the input state before performing the part corresponding to Fig. 1, and the final gates \mathbf{U}_{θ_2} and \mathbf{U}_R in Fig. 2 after the part corresponding to Fig. 1 are also different. This preprocessing implements the following transformation with sufficient precision $O(\Delta)$ to achieve the overall precision Δ

$$|\psi\rangle^X \otimes |0\rangle \otimes |0\rangle \otimes |0\rangle \otimes |0\rangle \otimes |0\rangle^{X'} \otimes |0\rangle^A \otimes |0\rangle^B \quad (100)$$

$$\xrightarrow{\text{CNOT}} \sum_{\tilde{x}} \alpha_{\tilde{x}} |\tilde{x}\rangle^X \otimes |0\rangle \otimes |0\rangle \otimes |0\rangle \otimes |0\rangle \otimes |\tilde{x}\rangle^{X'} \otimes |0\rangle^A \otimes |0\rangle^B \quad (101)$$

$$\begin{aligned} & \xrightarrow{\mathbf{F}_D^\dagger \otimes \mathcal{O}_\rho^\dagger \otimes \mathbf{R}_{\theta_3(\epsilon)}} \sum_{\tilde{x}} \alpha_{\tilde{x}} \mathbf{F}_D^\dagger |\tilde{x}\rangle^X \otimes |0\rangle \otimes |0\rangle \otimes |0\rangle \otimes |0\rangle \otimes \mathbf{U}_\rho^\dagger |\tilde{x}\rangle^{X'} \otimes \\ & \left(\sqrt{\frac{\epsilon/Q_{\max}^{(\tau)}}{1 + (\epsilon/Q_{\max}^{(\tau)})}} |0\rangle^A + \sqrt{\frac{1}{1 + (\epsilon/Q_{\max}^{(\tau)})}} |1\rangle^A \right) \otimes |0\rangle^B. \end{aligned} \quad (102)$$

In (101), we use $O(D \log(G))$ CNOT gates acting on each of the $O(D \log(G))$ qubits of the quantum registers X and X' . In (102), \mathbf{F}_D^\dagger is implemented by $O(D \log(G) \log \log(G) \text{polylog}(\frac{1}{\Delta}))$ gates as shown in (72), \mathcal{O}_ρ^\dagger takes time T_ρ , and a fixed one-qubit rotation $\mathbf{R}_{\theta_3(\epsilon)}$ defined as (85) is implemented with precision $O(\Delta)$ using $O(\text{polylog}(\frac{1}{\Delta}))$ gates (Nielsen & Chuang, 2011).

Then, after performing the same part as in Fig. 1, which is dominant, the circuit in Fig. 2 performs \mathbf{U}_{θ_2} defined as (98) and \mathbf{U}_R defined as (99). We can implement \mathbf{U}_{θ_2} in the same way as (91), i.e., \mathbf{U}_{θ_1} in Lemma 1, using $O(\text{polylog}(\frac{1}{\Delta}))$ gates. We can implement \mathbf{U}_R using $O(D \log(G) \text{polylog}(\frac{1}{\Delta}))$ gates since $|\theta\rangle$ is stored in $O(\text{polylog}(\frac{1}{\Delta}))$ qubits and $\mathcal{H}^{X'}$ consists of $O(D \log(G))$ qubits.

After performing \mathbf{U}_R , we perform a measurement of the last qubit B in the computational basis $\{|0\rangle^B, |1\rangle^B\}$. To calculate the probability of obtaining the outcome 0 in this measurement of B , suppose that we performed a measurement of the one-qubit register A in the computational basis $\{|0\rangle^A, |1\rangle^A\}$. Then, we would obtain the outcome $|0\rangle^A$ with probability $\frac{\epsilon/Q_{\max}^{(\tau)}}{1 + (\epsilon/Q_{\max}^{(\tau)})}$, and the outcome $|1\rangle^A$ with probability $\frac{1}{1 + (\epsilon/Q_{\max}^{(\tau)})}$. Conditioned on the outcome $|0\rangle^A$, the measurement of B yields the outcome $|0\rangle^B$ with probability 1 correspondingly to the first term of (99). Conditioned on $|1\rangle^A$, owing to the third term of (99), the measurement of B yields the outcome $|0\rangle^B$ with probability

$$\begin{aligned} & \sum_{\tilde{x}' \in \tilde{\mathcal{X}}} \left| \sum_{\tilde{x} \in \tilde{\mathcal{X}}} \alpha_{\tilde{x}} \langle \tilde{x}' | \mathbf{F}_D^\dagger | \tilde{x} \rangle \langle 0 | \mathbf{U}_\rho^\dagger | \tilde{x} \rangle \sqrt{\frac{1}{Q_{\max}^{(\tau)}} Q^{(\tau)} \left(\frac{\tilde{x}'}{G} \right)} \right|^2 \\ & = \sum_{\tilde{x}' \in \tilde{\mathcal{X}}} \frac{1}{Q_{\max}^{(\tau)}} Q^{(\tau)} \left(\frac{\tilde{x}'}{G} \right) \left| \sum_{\tilde{x} \in \tilde{\mathcal{X}}} \alpha_{\tilde{x}} \langle \tilde{x}' | \mathbf{F}_D^\dagger | \tilde{x} \rangle \langle 0 | \mathbf{U}_\rho^\dagger | \tilde{x} \rangle \right|^2. \end{aligned} \quad (103)$$

Note that the second term of (99) has no contribution in (103) because σ_x flips $|0\rangle$ to $|1\rangle$. Due to $|\langle 0 | \mathbf{U}_\rho^\dagger | \tilde{x} \rangle| = |\langle \tilde{x} | \left(\sum_{\tilde{x}'} \sqrt{\hat{q}^{(\rho)}(\tilde{x}')} |\tilde{x}'\rangle \right)| = \sqrt{\hat{q}^{(\rho)}(\tilde{x})}$, we have

$$\begin{aligned} (103) & = \sum_{\tilde{x}' \in \tilde{\mathcal{X}}} \frac{1}{Q_{\max}^{(\tau)}} Q^{(\tau)} \left(\frac{\tilde{x}'}{G} \right) \left| \sum_{\tilde{x} \in \tilde{\mathcal{X}}} \alpha_{\tilde{x}} \langle \tilde{x}' | \mathbf{F}_D^\dagger | \tilde{x} \rangle \sqrt{\hat{q}^{(\rho)}(\tilde{x})} \right|^2 \\ & = \sum_{\tilde{x}' \in \tilde{\mathcal{X}}} \frac{1}{Q_{\max}^{(\tau)}} Q^{(\tau)} \left(\frac{\tilde{x}'}{G} \right) \left| \sum_{\tilde{x} \in \tilde{\mathcal{X}}} \alpha_{\tilde{x}} \langle \tilde{x}' | \mathbf{F}_D^\dagger \sqrt{\hat{\mathbf{q}}^{(\rho)}} | \tilde{x} \rangle \right|^2. \end{aligned} \quad (104)$$

By definition (95) of $|\psi\rangle$, we have

$$\begin{aligned}
 (104) &= \sum_{\tilde{x}' \in \tilde{\mathcal{X}}} \frac{1}{Q_{\max}^{(\tau)}} Q^{(\tau)} \left(\frac{\tilde{x}'}{G} \right) \left| \langle \tilde{x}' | \mathbf{F}_D^\dagger \sqrt{\hat{\mathbf{q}}^{(\rho)}} | \psi \rangle \right|^2 \\
 &= \sum_{\tilde{x}' \in \tilde{\mathcal{X}}} \frac{1}{Q_{\max}^{(\tau)}} Q^{(\tau)} \left(\frac{\tilde{x}'}{G} \right) \langle \tilde{x}' | \mathbf{F}_D^\dagger \sqrt{\hat{\mathbf{q}}^{(\rho)}} | \psi \rangle \langle \psi | \sqrt{\hat{\mathbf{q}}^{(\rho)}} \mathbf{F}_D | \tilde{x}' \rangle \\
 &= \frac{1}{Q_{\max}^{(\tau)}} \text{Tr} \left[\mathbf{F}_D^\dagger \sqrt{\hat{\mathbf{q}}^{(\rho)}} | \psi \rangle \langle \psi | \sqrt{\hat{\mathbf{q}}^{(\rho)}} \mathbf{F}_D \left(\sum_{\tilde{x}' \in \tilde{\mathcal{X}}} Q^{(\tau)} \left(\frac{\tilde{x}'}{G} \right) | \tilde{x}' \rangle \langle \tilde{x}' | \right) \right]. \tag{105}
 \end{aligned}$$

By definition (41) of $\mathbf{Q}^{(\tau)}$ in Sec. B, we obtain

$$\begin{aligned}
 (105) &= \frac{1}{Q_{\max}^{(\tau)}} \text{Tr} \left[\mathbf{F}_D^\dagger \sqrt{\hat{\mathbf{q}}^{(\rho)}} | \psi \rangle \langle \psi | \sqrt{\hat{\mathbf{q}}^{(\rho)}} \mathbf{F}_D \mathbf{Q}^{(\tau)} \right] \\
 &= \frac{1}{Q_{\max}^{(\tau)}} \text{Tr} \left[| \psi \rangle \langle \psi | \sqrt{\hat{\mathbf{q}}^{(\rho)}} \mathbf{F}_D \mathbf{Q}^{(\tau)} \mathbf{F}_D^\dagger \sqrt{\hat{\mathbf{q}}^{(\rho)}} \right] \\
 &= \frac{1}{Q_{\max}^{(\tau)}} \text{Tr} \left[| \psi \rangle \langle \psi | \sqrt{\hat{\mathbf{q}}^{(\rho)}} \mathbf{k} \sqrt{\hat{\mathbf{q}}^{(\rho)}} \right], \tag{106}
 \end{aligned}$$

where the last equality follows from the perfect reconstruction of the kernel k shown in Proposition 1. Therefore, since a measurement of the auxiliary qubit \mathcal{H}^A in the computational basis $\{|0\rangle^A, |1\rangle^A\}$ yields outcome 0 and 1 with probability $\frac{\epsilon/Q_{\max}^{(\tau)}}{1+(\epsilon/Q_{\max}^{(\tau)})}$ and $\frac{1}{1+(\epsilon/Q_{\max}^{(\tau)})}$ respectively, the circuit in Fig. 2 yields the outcome 0 with probability

$$\begin{aligned}
 &\frac{\epsilon/Q_{\max}^{(\tau)}}{1+(\epsilon/Q_{\max}^{(\tau)})} \times 1 + \frac{1}{1+(\epsilon/Q_{\max}^{(\tau)})} \times \left(\frac{1}{Q_{\max}^{(\tau)}} \text{Tr} \left[| \psi \rangle \langle \psi | \sqrt{\hat{\mathbf{q}}^{(\rho)}} \mathbf{k} \sqrt{\hat{\mathbf{q}}^{(\rho)}} \right] \right) \\
 &= \frac{1}{1+(\epsilon/Q_{\max}^{(\tau)})} \times \text{Tr} \left[| \psi \rangle \langle \psi | \left(\frac{\epsilon}{Q_{\max}^{(\tau)}} \mathbb{1} \right) \right] + \frac{1}{1+(\epsilon/Q_{\max}^{(\tau)})} \times \text{Tr} \left[| \psi \rangle \langle \psi | \left(\frac{1}{Q_{\max}^{(\tau)}} \sqrt{\hat{\mathbf{q}}^{(\rho)}} \mathbf{k} \sqrt{\hat{\mathbf{q}}^{(\rho)}} \right) \right] \\
 &= \frac{1}{1+(\epsilon/Q_{\max}^{(\tau)})} \times \text{Tr} \left[| \psi \rangle \langle \psi | \left(\frac{1}{Q_{\max}^{(\tau)}} \sqrt{\hat{\mathbf{q}}^{(\rho)}} \mathbf{k} \sqrt{\hat{\mathbf{q}}^{(\rho)}} + \frac{\epsilon}{Q_{\max}^{(\tau)}} \mathbb{1} \right) \right] \\
 &= \text{Tr} \left[| \psi \rangle \langle \psi | \left(\frac{1}{1+(\epsilon/Q_{\max}^{(\tau)})} \hat{\Sigma}_\epsilon \right) \right], \tag{107}
 \end{aligned}$$

where the last equality follows from the definition (62) of $\hat{\Sigma}_\epsilon$ in Sec. C, which achieves (74) for $\Lambda = \frac{1}{1+(\epsilon/Q_{\max}^{(\tau)})} \hat{\Sigma}_\epsilon$ within a claimed runtime. \square

Using these block encodings in Lemmas 1 and 2, we prove Theorem 1 as follows.

Proof of Theorem 1. We prove that Algorithm 1 has the claimed runtime guarantee. The dominant step of Algorithm 1 is Step 5, as shown in the following.

In Step 2, after the initialization of $|0\rangle^X \otimes |0\rangle^{X'}$, we prepare $\sum_{\tilde{x} \in \tilde{\mathcal{X}}} |0\rangle^X \otimes \sqrt{\hat{\mathbf{q}}^{(\rho)}} |\tilde{x}\rangle^{X'}$ by one query to the oracle \mathcal{O}_ρ , followed by $O(D \log(G))$ CNOT gates to prepare $\sum_{\tilde{x} \in \tilde{\mathcal{X}}} |\tilde{x}\rangle^X \otimes \sqrt{\hat{\mathbf{q}}^{(\rho)}} |\tilde{x}\rangle^{X'}$, since \mathcal{H}^X consists of $O(D \log(G))$ qubits. Step 3 performs \mathbf{F}_D^\dagger , which is implemented using $O(D \log(G) \log \log(G) \text{polylog}(\frac{1}{\Delta}))$ gates as shown in (72). Step 4 is implemented by the block encoding of $\sqrt{\frac{1}{Q_{\max}^{(\tau)}} \mathbf{Q}^{(\tau)}}$ within time $O(D \log(G) \log \log(G) \text{polylog}(\frac{1}{\Delta}) + T_\tau)$ as shown

in Lemma 1. The runtime at this moment is $O(D \log(G) \log \log(G) \text{polylog}(\frac{1}{\Delta}) + T_\rho + T_\tau)$. After applying the block encoding of $\sqrt{\frac{1}{Q_{\max}^{(\tau)}}} \mathbf{Q}^{(\tau)}$, we obtain a quantum state represented as a linear combination including a term

$$\sum_{\tilde{x} \in \tilde{\mathcal{X}}} |\tilde{x}\rangle^X \otimes \sqrt{\frac{1}{Q_{\max}^{(\tau)}}} \mathbf{Q}^{(\tau)} \mathbf{F}_D^\dagger \sqrt{\hat{\mathbf{q}}^{(\rho)}} |\tilde{x}\rangle^{X'}, \quad (108)$$

and the norm of this term is

$$\begin{aligned} \left\| \sum_{\tilde{x} \in \tilde{\mathcal{X}}} |\tilde{x}\rangle^X \otimes \sqrt{\frac{1}{Q_{\max}^{(\tau)}}} \mathbf{Q}^{(\tau)} \mathbf{F}_D^\dagger \sqrt{\hat{\mathbf{q}}^{(\rho)}} |\tilde{x}\rangle^{X'} \right\|_2 &= \sqrt{\frac{\text{Tr} \left[\sqrt{\hat{\mathbf{q}}^{(\rho)}} \mathbf{F}_D \mathbf{Q}^{(\tau)} \mathbf{F}_D^\dagger \sqrt{\hat{\mathbf{q}}^{(\rho)}} \right]}{Q_{\max}^{(\tau)}}} = \sqrt{\frac{\text{Tr} \left[\mathbf{F}_D \mathbf{Q}^{(\tau)} \mathbf{F}_D^\dagger \hat{\mathbf{q}}^{(\rho)} \right]}{Q_{\max}^{(\tau)}}} \\ &= \sqrt{\frac{\text{Tr} \hat{\Sigma}}{Q_{\max}^{(\tau)}}}, \end{aligned} \quad (109)$$

where the last equality uses $\hat{\Sigma} = \mathbf{k}\hat{\mathbf{q}}^{(\rho)} = \mathbf{F}_D \mathbf{Q}^{(\tau)} \mathbf{F}_D^\dagger \hat{\mathbf{q}}^{(\rho)}$ obtained from Proposition 1. For any translation-invariant kernel $\tilde{k}(x', x) = \tilde{k}_{\text{TI}}(x' - x)$, we can evaluate $\text{Tr} \hat{\Sigma}$ as

$$\text{Tr} \hat{\Sigma} = \text{Tr} \left[\mathbf{k}\hat{\mathbf{q}}^{(\rho)} \right] = \tilde{k}_{\text{TI}}(0) \text{Tr} \hat{\mathbf{q}}^{(\rho)} = \tilde{k}(0, 0) = \Omega(1), \quad (110)$$

where we use the assumption $\tilde{k}(0, 0) = \Omega(k(0, 0)) = \Omega(1)$. Thus, to obtain the normalized quantum state proportional to the term (108), Step 4 is followed by amplitude amplification (Brassard et al., 2002), which repeats the above steps $O\left(\sqrt{\frac{Q_{\max}^{(\tau)}}{\text{Tr} \hat{\Sigma}}}\right) = O\left(\sqrt{Q_{\max}^{(\tau)}}\right)$ times. Therefore, at the end of Step 4 including the amplitude amplification, the runtime is

$$O\left(\left(D \log(G) \log \log(G) \text{polylog}\left(\frac{1}{\Delta}\right) + T_\rho + T_\tau\right) \times \sqrt{Q_{\max}^{(\tau)}}\right). \quad (111)$$

Step 5 is performed by implementing a block encoding of $\hat{\Sigma}_\epsilon^{-\frac{1}{2}}$, which is obtained from quantum singular value transformation (QSVT) (Gilyén et al., 2019) of the block encoding of $\frac{1}{1+(\epsilon/Q_{\max}^{(\tau)})} \hat{\Sigma}_\epsilon$ constructed in Lemma 2. The block encoding of $\frac{1}{1+(\epsilon/Q_{\max}^{(\tau)})} \hat{\Sigma}_\epsilon$ can be implemented in time $O(D \log(G) \log \log(G) \text{polylog}(\frac{1}{\Delta}) + T_\rho + T_\tau)$ as shown in Lemma 2. Then, the QSVT combined with variable-time amplitude amplification (Ambainis, 2012; Childs et al., 2017; Chakraborty et al., 2018) yields a block encoding of $\left(\frac{1}{1+(\epsilon/Q_{\max}^{(\tau)})} \hat{\Sigma}_\epsilon\right)^{-\frac{1}{2}}$, which can be applied to any given quantum state up to Δ precision using the block encoding of $\frac{1}{1+(\epsilon/Q_{\max}^{(\tau)})} \hat{\Sigma}_\epsilon$ repeatedly $\tilde{O}\left(\left(\frac{Q_{\max}^{(\tau)}}{\epsilon} + 1\right) \text{polylog}\left(\frac{1}{\Delta}\right)\right)$ times (Gilyén et al., 2019). This repetition includes the runtime required for the amplitude amplification, and $\frac{Q_{\max}^{(\tau)}}{\epsilon} + 1$ is the condition number of $\frac{1}{1+(\epsilon/Q_{\max}^{(\tau)})} \hat{\Sigma}_\epsilon$ since it holds that

$$\frac{1}{1+(\epsilon/Q_{\max}^{(\tau)})} \frac{\epsilon}{Q_{\max}^{(\tau)}} \mathbb{1} \leq \frac{1}{1+(\epsilon/Q_{\max}^{(\tau)})} \hat{\Sigma}_\epsilon \leq \mathbb{1}. \quad (112)$$

Thus, Step 5 including amplitude amplification can be implemented in time

$$\begin{aligned} &O\left(D \log(G) \log \log(G) \text{polylog}\left(\frac{1}{\Delta}\right) + T_\rho + T_\tau\right) \times \tilde{O}\left(\left(\frac{Q_{\max}^{(\tau)}}{\epsilon} + 1\right) \text{polylog}\left(\frac{1}{\Delta}\right)\right) \\ &= O(D \log(G) \log \log(G) + T_\rho + T_\tau) \times \tilde{O}\left(\frac{Q_{\max}^{(\tau)}}{\epsilon} \text{polylog}\left(\frac{1}{\Delta}\right)\right). \end{aligned} \quad (113)$$

Therefore from (111) and (113), we obtain the total runtime at the end of Step 5 including amplitude amplification

$$\begin{aligned} & O(D \log(G) \log \log(G) + T_\rho + T_\tau) \times \tilde{O} \left(\left(\sqrt{Q_{\max}^{(\tau)}} + \frac{Q_{\max}^{(\tau)}}{\epsilon} \right) \text{polylog} \left(\frac{1}{\Delta} \right) \right) \\ & = O(D \log(G) \log \log(G) + T_\rho + T_\tau) \times \tilde{O} \left(\frac{Q_{\max}^{(\tau)}}{\epsilon} \text{polylog} \left(\frac{1}{\Delta} \right) \right), \end{aligned} \quad (114)$$

which yields the conclusion. \square

E. Proof of Theorem 2

We prove Theorem 2 in the main text on the overall runtime of the supervised learning with optimized random features. To perform the SGD, recall the classical oracles

$$\mathcal{O}_{\tilde{x}}(n) = \tilde{x}_n, \quad \mathcal{O}_y(n) = y_n. \quad (115)$$

Proof of Theorem 2. We bound the runtime of each step of Algorithm 2. In Step 2, using Algorithm 1 repeatedly M times, we can obtain M optimized random features within time

$$O(MT_1), \quad (116)$$

where T_1 is the runtime of Algorithm 1 given by Theorem 1 in Sec. D. As for Step 4, we bound the runtime of the SGD in Algorithm 3. In the following, we show that the runtime of each iteration of the SGD is $O(MD + T_{\tilde{x}} + T_y)$, and the required number of iterations in the SGD is upper bounded by $O\left(\frac{1}{\epsilon^2 Q_{\min}^2} \log\left(\frac{1}{\delta}\right)\right)$.

We analyze the runtime of the t th iteration of the SGD for each $t \in \{0, \dots, T-1\}$. The dominant step in the t th iteration is the calculation of an unbiased estimate $\hat{g}^{(t)}$ of the gradient $\mathbb{E}[\hat{g}^{(t)}] = \nabla I(\alpha^{(t)})$ for

$$I(\alpha) := \sum_{\tilde{x} \in \tilde{\mathcal{X}}} p^{(\rho)}(\tilde{x}) \left| f(\tilde{x}) - \sum_{m=0}^{M-1} \alpha_m \varphi(v_m, \tilde{x}) \right|^2, \quad (117)$$

where $\varphi(v, x) = e^{-2\pi i v \cdot x}$, $p^{(\rho)}(\tilde{x}) = \int_{\Delta_{\tilde{x}}} d\rho(x)$, and we write

$$\alpha = \begin{pmatrix} \alpha_0 \\ \vdots \\ \alpha_{M-1} \end{pmatrix}. \quad (118)$$

The gradient of I is given by

$$\begin{aligned} \nabla I(\alpha) &= \sum_{\tilde{x} \in \tilde{\mathcal{X}}} p^{(\rho)}(\tilde{x}) \begin{pmatrix} 2\Re \left[e^{-2\pi i v_0 \cdot \tilde{x}} \left(f(\tilde{x}) - \sum_{m=0}^{M-1} \alpha_m e^{2\pi i v_m \cdot \tilde{x}} \right) \right] \\ \vdots \\ 2\Re \left[e^{-2\pi i v_{M-1} \cdot \tilde{x}} \left(f(\tilde{x}) - \sum_{m=0}^{M-1} \alpha_m e^{2\pi i v_m \cdot \tilde{x}} \right) \right] \end{pmatrix} \\ &= \sum_{m=0}^{M-1} \frac{1}{M} \sum_{\tilde{x} \in \tilde{\mathcal{X}}} p^{(\rho)}(\tilde{x}) \begin{pmatrix} 2\Re \left[e^{-2\pi i v_0 \cdot \tilde{x}} \left(f(\tilde{x}) - M\alpha_m e^{2\pi i v_m \cdot \tilde{x}} \right) \right] \\ \vdots \\ 2\Re \left[e^{-2\pi i v_{M-1} \cdot \tilde{x}} \left(f(\tilde{x}) - M\alpha_m e^{2\pi i v_m \cdot \tilde{x}} \right) \right] \end{pmatrix}, \end{aligned} \quad (119)$$

where \Re represents the real part. In the t th iteration, Algorithm 3 estimate the gradient at a point denoted by

$$\alpha^{(t)} = \begin{pmatrix} \alpha_0^{(t)} \\ \vdots \\ \alpha_{M-1}^{(t)} \end{pmatrix} \in \left\{ \alpha^{(1)}, \dots, \alpha^{(T)} \right\}. \quad (120)$$

Using a pair of given data points $(\tilde{x}_t, y_t = f(\tilde{x}_t)) \in \{(\tilde{x}_0, y_0), (\tilde{x}_1, y_1), \dots\}$ sampled with probability $p^{(\rho)}(\tilde{x})$ as observations of an independently and identically distributed (IID) random variable, and an integer $m \in \{0, \dots, M-1\}$ uniformly sampled with probability $\frac{1}{M}$, we give an unbiased estimate $\hat{g}^{(t)}$ of this gradient at each point $\alpha^{(t)}$ by

$$\hat{g}^{(t)} = \begin{pmatrix} 2\Re \left[e^{-2\pi i v_0 \cdot \tilde{x}_t} \left(y_t - M \alpha_m^{(t)} e^{2\pi i v_m \cdot \tilde{x}_t} \right) \right] \\ \vdots \\ 2\Re \left[e^{-2\pi i v_{M-1} \cdot \tilde{x}_t} \left(y_t - M \alpha_m^{(t)} e^{2\pi i v_m \cdot \tilde{x}_t} \right) \right] \end{pmatrix}. \quad (121)$$

By construction, we have

$$\mathbb{E} \left[\hat{g}^{(t)} \right] = \nabla I \left(\alpha^{(t)} \right). \quad (122)$$

We obtain \tilde{x}_t using the classical oracle $\mathcal{O}_{\tilde{x}}$ within time $T_{\tilde{x}}$, and $y_t = f(\tilde{x}_t)$ using the classical oracle \mathcal{O}_y within time T_y . As for m , since we can represent the integer m using $\lceil \log_2(M) \rceil$ bits, where $\lceil x \rceil$ is the least integer greater than or equal to x , we can sample m from a uniform distribution using a numerical library for generating a random number within time $O(\text{polylog}(M))$. Note that even in case it is expensive to use randomness in classical computation, quantum computation can efficiently sample m of $\lceil \log_2(M) \rceil$ bits from the uniform distribution within time $O(\log(M))$. In this quantum algorithm, $\lceil \log_2(M) \rceil$ qubits are initially prepared in $|0\rangle^{\otimes \lceil \log_2(M) \rceil}$, and the Hadamard gate $H = \frac{1}{\sqrt{2}} \begin{pmatrix} 1 & 1 \\ 1 & -1 \end{pmatrix}$ is applied to each qubit to obtain

$$\frac{1}{\sqrt{2^{\lceil \log_2(M) \rceil}}} (|0\rangle + |1\rangle)^{\otimes \lceil \log_2(M) \rceil}, \quad (123)$$

followed by a measurement of this state in the computational basis to obtain a $\lceil \log_2(M) \rceil$ -bit outcome sampled from the uniform distribution. Given \tilde{x}_t , y_t , and m , we can calculate each of the M element of \hat{g} in (121) within time $O(D)$ for calculating the inner product of D -dimensional vectors, and hence the calculation of all the M elements takes time $O(MD)$. Note that without sampling m , $O(M^2D)$ runtime per iteration would be needed, because each of the M elements of the gradient in (119) includes the sum over M terms. Therefore, each iteration takes time

$$O(T_{\tilde{x}} + T_y + \text{polylog}(M) + MD) = O(MD + T_{\tilde{x}} + T_y). \quad (124)$$

To bound the required number of iterations, we use an upper bound of the number of iterations in Algorithm 3 given in (Jain et al., 2019), which shows that if we have for any $\alpha \in \mathcal{W}$

$$\|\nabla I(\alpha)\|_2 \leq L, \quad (125)$$

the unbiased estimate \hat{g} for any point $\alpha \in \mathcal{W}$ almost surely satisfies

$$\|\hat{g}\|_2 \leq L, \quad (126)$$

and the diameter of \mathcal{W} is bounded by

$$\text{diam } \mathcal{W} \leq d, \quad (127)$$

then, after T iterations, with high probability greater than $1 - \delta$, Algorithm 3 returns α satisfying

$$\epsilon = O \left(dL \sqrt{\frac{\log(\frac{1}{\delta})}{T}} \right), \quad (128)$$

where we write

$$\epsilon = I(\alpha) - \min_{\alpha \in \mathcal{W}} \{I(\alpha)\}. \quad (129)$$

In the following, we bound d and L in (128) to clarify the upper bound of the required number of iterations T in our setting.

To show a bound of d , recall the assumption that we are given a sufficiently large number M of features for achieving the learning in our setting. Then, Bach (2017) has shown that with the M features sampled from the weighted probability distribution $Q(v_m)P^{(\tau)}(v_m)$ by Algorithm 1, the learning to the accuracy $O(\epsilon)$ can be achieved with coefficients satisfying

$$\|\beta\|_2^2 = O \left(\frac{1}{M} \right), \quad (130)$$

where $\beta = (\beta_0, \dots, \beta_{M-1})^T$ is defined for each m as

$$\beta_m = \sqrt{Q(v_m)}\alpha_m. \quad (131)$$

This bound yields

$$\sum_{m=0}^{M-1} Q(v_m)\alpha_m^2 = O\left(\frac{1}{M}\right). \quad (132)$$

In the worst case, a lower bound of the left-hand side is

$$\sum_{m=0}^{M-1} Q(v_m)\alpha_m^2 \geq Q_{\min} \|\alpha\|_2^2, \quad (133)$$

where Q_{\min} is given by

$$Q_{\min} = \min \{Q(v_m) : m \in \{0, 1, \dots, M-1\}\}. \quad (134)$$

Note that as discussed in the main text, in the parameter region of sampling optimized random features that are weighted by importance and that nearly minimize M , the minimal weight Q_{\min} of these features is expected to be sufficiently large compared to ϵ , not dominating the runtime, while we include Q_{\min} in our analysis to bound the worst-case runtime. From (132) and (133), we obtain an upper bound of the norm of α minimizing I

$$\|\alpha\|_2^2 = O\left(\frac{1}{MQ_{\min}}\right). \quad (135)$$

Thus, it suffices to choose the parameter region \mathcal{W} of α as an M -dimensional ball of center 0 and of radius $O\left(\frac{1}{\sqrt{MQ_{\min}}}\right)$, which yields the diameter

$$d = O\left(\frac{1}{\sqrt{MQ_{\min}}}\right). \quad (136)$$

As for a bound of L , we obtain from (121)

$$\|\hat{g}\|_2 = O\left(M\|\alpha\|_2 + \sqrt{M}\right) = O\left(\sqrt{\frac{M}{Q_{\min}}} + \sqrt{M}\right) = O\left(\sqrt{\frac{M}{Q_{\min}}}\right), \quad (137)$$

where we take the worst case of small Q_{\min} , and we use bounds

$$\sqrt{\sum_{m=0}^{M-1} |M\alpha_m e^{2\pi i v_m \cdot \hat{x}_t}|^2} = O(M\|\alpha\|_2), \quad (138)$$

$$\sqrt{\sum_{m=0}^{M-1} y_t^2} = O(\sqrt{M}). \quad (139)$$

Since this upper bound of $\|\hat{g}\|_2$ is larger than $\|\nabla I(\alpha)\|_2$, we have

$$L = O\left(\sqrt{\frac{M}{Q_{\min}}}\right). \quad (140)$$

Using (136) and (140), we bound the right-hand side of (128)

$$\epsilon = O\left(dL\sqrt{\frac{\log\left(\frac{1}{\delta}\right)}{T}}\right) = O\left(\frac{1}{Q_{\min}}\sqrt{\frac{\log\left(\frac{1}{\delta}\right)}{T}}\right). \quad (141)$$

Therefore, it follows that

$$T = O\left(\frac{1}{\epsilon^2 Q_{\min}^2} \log\left(\frac{1}{\delta}\right)\right). \quad (142)$$

Combining (116), (124), and (142), we obtain the claimed overall runtime.

□

References

- Aaronson, S. Read the fine print. *Nature Physics*, 11(4):291, 2015. URL <https://www.nature.com/articles/nphys3272>.
- Alaoui, A. and Mahoney, M. W. Fast randomized kernel ridge regression with statistical guarantees. In Cortes, C., Lawrence, N. D., Lee, D. D., Sugiyama, M., and Garnett, R. (eds.), *Advances in Neural Information Processing Systems 28*, pp. 775–783. Curran Associates, Inc., 2015. URL <http://papers.nips.cc/paper/5716-fast-randomized-kernel-ridge-regression-with-statistical-guarantees.pdf>.
- Ambainis, A. Variable time amplitude amplification and quantum algorithms for linear algebra problems. In *29th International Symposium on Theoretical Aspects of Computer Science, STACS 2012, February 29th - March 3rd, 2012, Paris, France*, pp. 636–647, 2012. doi: 10.4230/LIPIcs.STACS.2012.636. URL <https://drops.dagstuhl.de/opus/volltexte/2012/3426/>.
- Arute, F., Arya, K., Babbush, R., Bacon, D., Bardin, J. C., Barends, R., Biswas, R., Boixo, S., Brandao, F. G., Buell, D. A., et al. Quantum supremacy using a programmable superconducting processor. *Nature*, 574(7779):505–510, 2019. URL <https://www.nature.com/articles/s41586-019-1666-5>.
- Avron, H., Sindhvani, V., Yang, J., and Mahoney, M. W. Quasi-monte carlo feature maps for shift-invariant kernels. *Journal of Machine Learning Research*, 17(120):1–38, 2016. URL <http://jmlr.org/papers/v17/14-538.html>.
- Avron, H., Kapralov, M., Musco, C., Musco, C., Velingker, A., and Zandieh, A. Random Fourier features for kernel ridge regression: Approximation bounds and statistical guarantees. In Precup, D. and Teh, Y. W. (eds.), *Proceedings of the 34th International Conference on Machine Learning*, volume 70 of *Proceedings of Machine Learning Research*, pp. 253–262, International Convention Centre, Sydney, Australia, 06–11 Aug 2017. PMLR. URL <http://proceedings.mlr.press/v70/avron17a.html>.
- Bach, F. Sharp analysis of low-rank kernel matrix approximations. In Shalev-Shwartz, S. and Steinwart, I. (eds.), *Proceedings of the 26th Annual Conference on Learning Theory*, volume 30 of *Proceedings of Machine Learning Research*, pp. 185–209, Princeton, NJ, USA, 12–14 Jun 2013. PMLR. URL <http://proceedings.mlr.press/v30/Bach13.html>.
- Bach, F. On the equivalence between kernel quadrature rules and random feature expansions. *Journal of Machine Learning Research*, 18(21):1–38, 2017. URL <http://jmlr.org/papers/v18/15-178.html>.
- Biamonte, J., Wittek, P., Pancotti, N., Rebentrost, P., Wiebe, N., and Lloyd, S. Quantum machine learning. *Nature*, 549(7671):195, 2017. URL <https://www.nature.com/articles/nature23474>.
- Brassard, G., Høyer, P., Mosca, M., and Tapp, A. *Quantum amplitude amplification and estimation*, volume 305, pp. 53–74. AMS Contemporary Mathematics, 2002. URL <http://www.ams.org/books/conm/305/>.
- Carratino, L., Rudi, A., and Rosasco, L. Learning with sgd and random features. In Bengio, S., Wallach, H., Larochelle, H., Grauman, K., Cesa-Bianchi, N., and Garnett, R. (eds.), *Advances in Neural Information Processing Systems 31*, pp. 10192–10203. Curran Associates, Inc., 2018. URL <http://papers.nips.cc/paper/8222-learning-with-sgd-and-random-features.pdf>.
- Chakraborty, S., Gilyén, A., and Jeffery, S. The power of block-encoded matrix powers: improved regression techniques via faster hamiltonian simulation. arXiv:1804.01973, Apr 2018. URL <https://arxiv.org/abs/1804.01973>.
- Chang, W.-C., Li, C.-L., Yang, Y., and Póczos, B. Data-driven random fourier features using stein effect. In *Proceedings of the Twenty-Sixth International Joint Conference on Artificial Intelligence, IJCAI-17*, pp. 1497–1503, 2017. doi: 10.24963/ijcai.2017/207. URL <https://www.ijcai.org/Proceedings/2017/207>.
- Chia, N.-H., Gilyén, A., Li, T., Lin, H.-H., Tang, E., and Wang, C. Sampling-based sublinear low-rank matrix arithmetic framework for dequantizing quantum machine learning. arXiv:1910.06151, Oct 2019. URL <https://arxiv.org/abs/1910.06151>.

- Childs, A. M., Kothari, R., and Somma, R. D. Quantum algorithm for systems of linear equations with exponentially improved dependence on precision. *SIAM Journal on Computing*, 46(6):1920–1950, 2017. URL <https://epubs.siam.org/doi/10.1137/16M1087072>.
- Ciliberto, C., Herbster, M., Ialongo, A. D., Pontil, M., Rocchetto, A., Severini, S., and Wossnig, L. Quantum machine learning: a classical perspective. *Proceedings of the Royal Society A: Mathematical, Physical and Engineering Sciences*, 474(2209):20170551, 2018. doi: 10.1098/rspa.2017.0551. URL <https://royalsocietypublishing.org/doi/abs/10.1098/rspa.2017.0551>.
- Cucker, F. and Smale, S. On the mathematical foundations of learning. *Bulletin of the American Mathematical Society*, 39:1–49, 2002. URL <https://www.ams.org/journals/bull/2002-39-01/S0273-0979-01-00923-5/#Additional>.
- Dai, B., Xie, B., He, N., Liang, Y., Raj, A., Balcan, M.-F. F., and Song, L. Scalable kernel methods via doubly stochastic gradients. In Ghahramani, Z., Welling, M., Cortes, C., Lawrence, N. D., and Weinberger, K. Q. (eds.), *Advances in Neural Information Processing Systems 27*, pp. 3041–3049. Curran Associates, Inc., 2014. URL <http://papers.nips.cc/paper/5238-scalable-kernel-methods-via-doubly-stochastic-gradients.pdf>.
- de Wolf, R. Quantum computing: Lecture notes. arXiv:1907.09415, Jul 2019. URL <https://arxiv.org/abs/1907.09415>.
- Dunjko, V. and Briegel, H. J. Machine learning & artificial intelligence in the quantum domain: a review of recent progress. *Reports on Progress in Physics*, 81(7):074001, jun 2018. doi: 10.1088/1361-6633/aab406. URL <https://iopscience.iop.org/article/10.1088/1361-6633/aab406>.
- Fine, S. and Scheinberg, K. Efficient svm training using low-rank kernel representations. *Journal of Machine Learning Research*, 2:243264, March 2002. ISSN 1532-4435. URL <http://www.jmlr.org/papers/v2/fine01a.html>.
- Gilyén, A., Su, Y., Low, G. H., and Wiebe, N. Quantum singular value transformation and beyond: Exponential improvements for quantum matrix arithmetics. In *Proceedings of the 51st Annual ACM SIGACT Symposium on Theory of Computing, STOC 2019*, pp. 193204, New York, NY, USA, 2019. Association for Computing Machinery. ISBN 9781450367059. doi: 10.1145/3313276.3316366. URL <https://dl.acm.org/doi/10.1145/3313276.3316366>.
- Giovannetti, V., Lloyd, S., and Maccone, L. Architectures for a quantum random access memory. *Phys. Rev. A*, 78:052310, Nov 2008a. doi: 10.1103/PhysRevA.78.052310. URL <https://link.aps.org/doi/10.1103/PhysRevA.78.052310>.
- Giovannetti, V., Lloyd, S., and Maccone, L. Quantum random access memory. *Phys. Rev. Lett.*, 100:160501, Apr 2008b. doi: 10.1103/PhysRevLett.100.160501. URL <https://link.aps.org/doi/10.1103/PhysRevLett.100.160501>.
- Grover, L. and Rudolph, T. Creating superpositions that correspond to efficiently integrable probability distributions. arXiv:quant-ph/0208112, Aug 2002. URL <https://arxiv.org/abs/quant-ph/0208112>.
- Hales, L. and Hallgren, S. Improved quantum fourier transform algorithm and applications. *Annual Symposium on Foundations of Computer Science - Proceedings*, pp. 515–525, 12 2000. ISSN 0272-5428. URL <https://pennstate.pure.elsevier.com/en/publications/improved-quantum-fourier-transform-algorithm-and-applications>.
- Häner, T., Roetteler, M., and Svore, K. M. Optimizing quantum circuits for arithmetic. arXiv:1805.12445, May 2018. URL <https://arxiv.org/abs/1805.12445>.
- Hann, C. T., Zou, C.-L., Zhang, Y., Chu, Y., Schoelkopf, R. J., Girvin, S. M., and Jiang, L. Hardware-efficient quantum random access memory with hybrid quantum acoustic systems. *Phys. Rev. Lett.*, 123:250501, Dec 2019. doi: 10.1103/PhysRevLett.123.250501. URL <https://link.aps.org/doi/10.1103/PhysRevLett.123.250501>.
- Harrow, A. W., Hassidim, A., and Lloyd, S. Quantum algorithm for linear systems of equations. *Phys. Rev. Lett.*, 103:150502, Oct 2009. doi: 10.1103/PhysRevLett.103.150502. URL <https://link.aps.org/doi/10.1103/PhysRevLett.103.150502>.

- Harvey, D. and Van Der Hoeven, J. Integer multiplication in time $O(n \log n)$. preprint, March 2019. URL <https://hal.archives-ouvertes.fr/hal-02070778>.
- Havlíček, V., Córcoles, A. D., Temme, K., Harrow, A. W., Kandala, A., Chow, J. M., and Gambetta, J. M. Supervised learning with quantum-enhanced feature spaces. *Nature*, 567(7747):209, 2019. URL <https://www.nature.com/articles/s41586-019-0980-2>.
- Jain, P., Nagaraj, D., and Netrapalli, P. Making the last iterate of sgd information theoretically optimal. In Beygelzimer, A. and Hsu, D. (eds.), *Proceedings of the Thirty-Second Conference on Learning Theory*, volume 99 of *Proceedings of Machine Learning Research*, pp. 1752–1755, Phoenix, USA, 25–28 Jun 2019. PMLR. URL <http://proceedings.mlr.press/v99/jain19a.html>.
- Jethwani, D., Le Gall, F., and Singh, S. K. Quantum-inspired classical algorithms for singular value transformation. arXiv:1910.05699, Oct 2019. URL <https://arxiv.org/abs/1910.05699>.
- Jiang, N., Pu, Y.-F., Chang, W., Li, C., Zhang, S., and Duan, L.-M. Experimental realization of 105-qubit random access quantum memory. *npj Quantum Information*, 5(1):28, 2019. URL <https://www.nature.com/articles/s41534-019-0144-0>.
- Kerenidis, I. and Prakash, A. Quantum Recommendation Systems. In Papadimitriou, C. H. (ed.), *8th Innovations in Theoretical Computer Science Conference (ITCS 2017)*, volume 67 of *Leibniz International Proceedings in Informatics (LIPIcs)*, pp. 49:1–49:21, Dagstuhl, Germany, 2017. Schloss Dagstuhl–Leibniz-Zentrum fuer Informatik. ISBN 978-3-95977-029-3. doi: 10.4230/LIPIcs.ITCS.2017.49. URL <http://drops.dagstuhl.de/opus/volltexte/2017/8154>.
- Le, Q., Sarlos, T., and Smola, A. Fastfood - computing hilbert space expansions in loglinear time. In Dasgupta, S. and McAllester, D. (eds.), *Proceedings of the 30th International Conference on Machine Learning*, volume 28 of *Proceedings of Machine Learning Research*, pp. 244–252, Atlanta, Georgia, USA, 17–19 Jun 2013. PMLR. URL <http://proceedings.mlr.press/v28/le13.html>.
- Li, Z., Ton, J.-F., Oglic, D., and Sejdinovic, D. Towards a unified analysis of random Fourier features. In Chaudhuri, K. and Salakhutdinov, R. (eds.), *Proceedings of the 36th International Conference on Machine Learning*, volume 97 of *Proceedings of Machine Learning Research*, pp. 3905–3914, Long Beach, California, USA, 09–15 Jun 2019. PMLR. URL <http://proceedings.mlr.press/v97/li19k.html>.
- Liu, F., Huang, X., Chen, Y., Yang, J., and Suykens, J. A. Random fourier features via fast surrogate leverage weighted sampling. arXiv:1911.09158, Nov 2019. URL <https://arxiv.org/abs/1911.09158>.
- Lloyd, S., Mohseni, M., and Rebentrost, P. Quantum principal component analysis. *Nature Physics*, 10(9):631, 2014. URL <https://www.nature.com/articles/nphys3029>.
- Lloyd, S., Garnerone, S., and Zanardi, P. Quantum algorithms for topological and geometric analysis of data. *Nature communications*, 7:10138, 2016. URL <https://www.nature.com/articles/ncomms10138>.
- Mengoni, R. and Di Pierro, A. Kernel methods in quantum machine learning. *Quantum Machine Intelligence*, 1(3): 65–71, Dec 2019. ISSN 2524-4914. doi: 10.1007/s42484-019-00007-4. URL <https://link.springer.com/article/10.1007/s42484-019-00007-4>.
- Montanaro, A. Quantum algorithms: an overview. *npj Quantum Information*, 2(1):1–8, 2016. URL <https://www.nature.com/articles/npjqi201523>.
- Nielsen, M. A. and Chuang, I. L. *Quantum Computation and Quantum Information: 10th Anniversary Edition*. Cambridge University Press, 10th edition, 2011. ISBN 9781107002173.
- Proakis, J. G. *Digital signal processing: principles algorithms and applications*. Pearson Education India, 2001.
- Rahimi, A. and Recht, B. Random features for large-scale kernel machines. In Platt, J. C., Koller, D., Singer, Y., and Roweis, S. T. (eds.), *Advances in Neural Information Processing Systems 20*, pp. 1177–1184. Curran Associates, Inc., 2008. URL <http://papers.nips.cc/paper/3182-random-features-for-large-scale-kernel-machines.pdf>.

- Rahimi, A. and Recht, B. Weighted sums of random kitchen sinks: Replacing minimization with randomization in learning. In Koller, D., Schuurmans, D., Bengio, Y., and Bottou, L. (eds.), *Advances in Neural Information Processing Systems 21*, pp. 1313–1320. Curran Associates, Inc., 2009. URL <http://papers.nips.cc/paper/3495-weighted-sums-of-random-kitchen-sinks-replacing-minimization-with-randomization-in-learning.pdf>.
- Rebentrost, P., Mohseni, M., and Lloyd, S. Quantum support vector machine for big data classification. *Phys. Rev. Lett.*, 113:130503, Sep 2014. doi: 10.1103/PhysRevLett.113.130503. URL <https://link.aps.org/doi/10.1103/PhysRevLett.113.130503>.
- Rudi, A. and Rosasco, L. Generalization properties of learning with random features. In Guyon, I., Luxburg, U. V., Bengio, S., Wallach, H., Fergus, R., Vishwanathan, S., and Garnett, R. (eds.), *Advances in Neural Information Processing Systems 30*, pp. 3215–3225. Curran Associates, Inc., 2017. URL <http://papers.nips.cc/paper/6914-generalization-properties-of-learning-with-random-features.pdf>.
- Rudi, A., Calandriello, D., Carratino, L., and Rosasco, L. On fast leverage score sampling and optimal learning. In Bengio, S., Wallach, H., Larochelle, H., Grauman, K., Cesa-Bianchi, N., and Garnett, R. (eds.), *Advances in Neural Information Processing Systems 31*, pp. 5672–5682. Curran Associates, Inc., 2018. URL <http://papers.nips.cc/paper/7810-on-fast-leverage-score-sampling-and-optimal-learning.pdf>.
- Schölkopf, B. and Smola, A. J. *Learning with Kernels: Support Vector Machines, Regularization, Optimization, and Beyond*. MIT Press, Cambridge, MA, USA, 2001. ISBN 0262194759.
- Shahrampour, S. and Kolouri, S. On sampling random features from empirical leverage scores: Implementation and theoretical guarantees. arXiv:1903.08329, Mar 2019. URL <https://arxiv.org/abs/1903.08329>.
- Shannon, C. E. Communication in the presence of noise. *Proceedings of the IRE*, 37(1):10–21, Jan 1949. ISSN 2162-6634. doi: 10.1109/JRPROC.1949.232969. URL <https://ieeexplore.ieee.org/abstract/document/1697831>.
- Shor, P. W. Polynomial-time algorithms for prime factorization and discrete logarithms on a quantum computer. *SIAM J. Comput.*, 26(5):14841509, October 1997. ISSN 0097-5397. doi: 10.1137/S0097539795293172. URL <https://epubs.siam.org/doi/10.1137/S0097539795293172>.
- Sinha, A. and Duchi, J. C. Learning kernels with random features. In Lee, D. D., Sugiyama, M., Luxburg, U. V., Guyon, I., and Garnett, R. (eds.), *Advances in Neural Information Processing Systems 29*, pp. 1298–1306. Curran Associates, Inc., 2016. URL <http://papers.nips.cc/paper/6180-learning-kernels-with-random-features.pdf>.
- Smola, A. J. and Schölkopf, B. Sparse greedy matrix approximation for machine learning. In *Proceedings of the Seventeenth International Conference on Machine Learning*, ICML 00, pp. 911918, San Francisco, CA, USA, 2000. Morgan Kaufmann Publishers Inc. ISBN 1558607072. URL <https://dl.acm.org/doi/10.5555/645529.657980>.
- Subramanian, S., Brierley, S., and Jozsa, R. Implementing smooth functions of a hermitian matrix on a quantum computer. *Journal of Physics Communications*, 3(6):065002, jun 2019. doi: 10.1088/2399-6528/ab25a2. URL <https://iopscience.iop.org/article/10.1088/2399-6528/ab25a2>.
- Sun, Y., Gilbert, A., and Tewari, A. But how does it work in theory? linear svm with random features. In Bengio, S., Wallach, H., Larochelle, H., Grauman, K., Cesa-Bianchi, N., and Garnett, R. (eds.), *Advances in Neural Information Processing Systems 31*, pp. 3379–3388. Curran Associates, Inc., 2018. URL <http://papers.nips.cc/paper/7598-but-how-does-it-work-in-theory-linear-svm-with-random-features.pdf>.
- Tang, E. A quantum-inspired classical algorithm for recommendation systems. In *Proceedings of the 51st Annual ACM SIGACT Symposium on Theory of Computing*, STOC 2019, pp. 217228, New York, NY, USA, 2019. Association for Computing Machinery. ISBN 9781450367059. doi: 10.1145/3313276.3316310. URL <https://doi.org/10.1145/3313276.3316310>.

- Ullah, E., Mianjy, P., Marinov, T. V., and Arora, R. Streaming kernel pca with tilde $o(\sqrt{n})$ random features. In Bengio, S., Wallach, H., Larochelle, H., Grauman, K., Cesa-Bianchi, N., and Garnett, R. (eds.), *Advances in Neural Information Processing Systems 31*, pp. 7311–7321. Curran Associates, Inc., 2018. URL <http://papers.nips.cc/paper/7961-streaming-kernel-pca-with-tildeosqrtn-random-features.pdf>.
- Wiebe, N., Braun, D., and Lloyd, S. Quantum algorithm for data fitting. *Phys. Rev. Lett.*, 109:050505, Aug 2012. doi: 10.1103/PhysRevLett.109.050505. URL <https://link.aps.org/doi/10.1103/PhysRevLett.109.050505>.
- Williams, C. K. I. and Seeger, M. Using the nystrom method to speed up kernel machines. In Leen, T. K., Dietterich, T. G., and Tresp, V. (eds.), *Advances in Neural Information Processing Systems 13*, pp. 682–688. MIT Press, 2001. URL <http://papers.nips.cc/paper/1866-using-the-nystrom-method-to-speed-up-kernel-machines.pdf>.
- Wossnig, L., Zhao, Z., and Prakash, A. Quantum linear system algorithm for dense matrices. *Phys. Rev. Lett.*, 120:050502, Jan 2018. doi: 10.1103/PhysRevLett.120.050502. URL <https://link.aps.org/doi/10.1103/PhysRevLett.120.050502>.
- Yu, F. X. X., Suresh, A. T., Choromanski, K. M., Holtmann-Rice, D. N., and Kumar, S. Orthogonal random features. In Lee, D. D., Sugiyama, M., Luxburg, U. V., Guyon, I., and Garnett, R. (eds.), *Advances in Neural Information Processing Systems 29*, pp. 1975–1983. Curran Associates, Inc., 2016. URL <http://papers.nips.cc/paper/6246-orthogonal-random-features.pdf>.
- Zhao, Z., Fitzsimons, J. K., and Fitzsimons, J. F. Quantum-assisted gaussian process regression. *Phys. Rev. A*, 99:052331, May 2019. doi: 10.1103/PhysRevA.99.052331. URL <https://link.aps.org/doi/10.1103/PhysRevA.99.052331>.